Research Square

Preprints are preliminary reports that have not undergone peer review.
They should not be considered conclusive, used to inform clinical practice,
or referenced by the media as validated information.

Translational Pharmacokinetic-Pharmacodynamic Modeling Framework for Protein Degraders in Oncology Drug Discovery

Massimiliano Fonsi

massimiliano.fonsi@evotec.com

Evotec (France) Sas

Radha Ramakrishnan

Dermot F. McGinnity

Research Article

Keywords:

Posted Date: May 20th, 2026

DOI: https://doi.org/10.21203/rs.3.rs-9608343/v1

License: This work is licensed under a Creative Commons Attribution 4.0 International License.
Read Full License

Additional Declarations: No competing interests reported.

Translational Pharmacokinetic-Pharmacodynamic Modeling Framework for Protein Degraders in Oncology Drug Discovery

Massimiliano Fonsi[1], Radha Ramakrishnan[2] and Dermot F. McGinnity[3]

[1]Evotec (France) Sas, 31100 Toulouse France.

[2]Bristol Myers Squibb, 10300 Campus Point Drive, San Diego, California, USA

[3]Evotec (Verona) Srl, 37135 Verona Italy.

Corresponding authors:

Massimiliano Fonsi, massimiliano.fonsi@evotec.com

0000-0003-4549-1483

The authors have no relevant financial or non-financial interests to disclose.

The authors have no competing interests to declare that are relevant to the content of this article.

Abstract

Many promising protein targets with potential therapeutic applications in oncology are challenging to modulate because they are non-enzymes lacking well defined active sites that are difficult to target using traditional occupancy-driven small molecules. Targeted protein (TP) degradation, the process of selectively degrading proteins, is a promising alternative therapeutic mode of action that can tag previously undruggable proteins towards degradation by the cell's proteasome.

A thorough understanding of the pre-clinical pharmacokinetic/pharmacodynamic (PK/PD) relationship is essential as a foundation for optimization and selection of quality candidate drugs and to develop a quantitative translational clinical framework. Such an analysis can guide early clinical dose selection and regimens, prioritise relevant combination therapies and identify patient cohorts most likely to respond with an acceptable therapeutic index. Building on this pre-clinical knowledge with clinical PK/PD and safety data facilitates optimization of dosing regimens and avoids excessive exposure in subsequent clinical studies.

The mechanisms of action of TPDs (target protein degraders) are stimulating the contribution and creativity of the modeling and simulation (M&S) community, developing mathematical models that inform experimental non-clinical and translational strategies for TP degradation drug discovery projects. Much of the PK/PD published literature in this field has investigated the link between PK and TP degradation but an essential part of the mechanism of action of degraders in oncology requires linking TP modulation to tumour cell kill and to biomarkers of efficacy and toxicity.

The methodology reported here describes a novel approach to deconvolute the TP degradation effect in two key steps: 1) modelling of drug dependent target protein degradation and 2) quantitatively describing the TP modulation vs tumour cell kill (and/or vs secondary biomarker) relationships across multiple in vivo tumour models. Case studies exemplify our modelling strategy for TPDs in oncology drug discovery and the use for translational purposes.

Abbreviations

bid = *bis in die* (twice a day); CDX = Cell line-derived xenograft; IVIVC = *in vitro-in vivo* correlation; mgd = molecular glue degrader; MoA = mechanism of action; NHP = non-human primate; PK/PD = pharmacokinetics and pharmacodynamics; PROTACs = proteolysis-targeting chimeras drugs; qd = *quaque die* (once a day); SM = small molecule; ss = steady state; TGI = tumour growth inhibition; TP = target protein; TPD = target protein degrader; TPf =target protein fraction remaining, tumour volume = TV.

Introduction

Conventional small molecule (SM) therapeutics elicit their effect via a specific drug-induced modulation of the activity of proteins such as enzymes, receptors, transporters or ion channels. However, the absolute requirement for well-defined SM binding sites renders about 80% of the proteome "undruggable"[1] (Dang et al. 2017) via this approach.

Chemically induced proximity between endogenous enzymes such as E3 ligases and an intracellular protein of interest can lead to post-translational modification and subsequent proteasomal degradation of the TP with biological and potentially therapeutic sequalae. Through a TP degradation mechanism, therapeutic approaches are not restricted to the agonistic/antagonistic SM mode of action, thus significantly expanding the range of the druggable proteome[2]. (Békés et al. 2022).

An additional advantage of TPDs arises because they do not necessarily bind to the catalytic site of enzymes which are typically well preserved among different isoenzymes of the same family. Thus, relative to the challenge of achieving exquisite isoform selectivity for classic SM protein inhibitors, TPDs may offer increased opportunity for selectivity and reduced promiscuity. In addition, due to their catalytic mechanism, where a single TPD molecule can induce the degradation of multiple TP molecules, this sub-stoichiometric effect can lead, at least in theory, to lower unbound concentrations relative to the levels required for traditional occupancy driven SM inhibitors, thus leading to potentially enhanced therapeutic indices. Whether more selective and tolerable profiles manifest clinically is yet to emerge for TPDs.

Proteolysis targeting chimeras (PROTACs) are bifunctional molecules consisting of two different ligands connected by a linker: one ligand binds to the TP and the other to an E3 ubiquitin ligase. The formation of this ternary complex brings the TP in proximity to the E3 ligase, triggering its ubiquitination and subsequent degradation by the proteasome[3,4] (Pettersson et al. - 2019, Deshaies -2015). Molecular glues, instead, are monovalent SM that rely on the secondary structural characteristics of the TP to facilitate the stabilization of protein-protein interactions. Similarly to what is achievable using bivalent PROTACs, the molecular glue induced complexes can cause changes in a series of biological functions including protein degradation. Given their monovalent nature, molecular glues may not face, to the same extent, the same challenges confronted with bivalent PROTACs, typically exhibiting a set of 'beyond Rule of 5' (bRo5) physicochemical properties such as large molecular weight and excess number of hydrogen bond donors and high lipophilicity. These properties of PROTACs can lead to significant practical experimental challenges such as high non-specific binding to plasticware and insolubility in addition to fundamental limitations in in vivo oral bioavailability[3,5] (Pettersson et al. – 2019, Pike et al. - 2020).

TPDs have experienced rapid progress in the industry's portfolio of candidate drugs, notably with the phase I trial in 2019 for ARV-110, developed by Arvinas, for the treatment of metastatic castration-resistant prostate cancer[6,7] (Yedla et al. – 2023). Currently, at least 18 TPDs are in phase I and I/II clinical trials for various tumour types, with a phase III trial of the ER degrader ARV-471 (https://www.arvinas.com/research-and-development/pipeline/) initiated in 2022[8] (Chirnomas et al. – 2023)

As more biological systems are tested, where different degraders and novel targets are investigated, it has become increasingly clear that achieving degradation of the target protein in an in vitro system is only the first critical milestone in a degrader discovery program[9]. (Riching et al. – 2022). Rather, highly efficacious degraders require a combination of multiple optimized parameters: normally consisting of rapid rate of degradation, high potency (DC_{50}, the compound concentration achieving half maximal degradation rate), high maximal degradation (Y_{min}, the minimal residual TP achievable), and sustained loss of target in the absence of re-dosing. Success in meeting these goals hinges upon the ability to quantitatively characterize and understand the dynamic cellular degradation profiles and relate them to the underlying mechanism for a TP treated with a defined concentration of TPD. From this foundation, compound properties can be optimized versus the defined TP properties via calibration of the desired rate, extent, duration and selectivity of TP degradation to achieve the desired phenotypic effect of cell kill to drive tumour regression with the promise of a sufficient therapeutic window.

An important parameter for TPDs is the rate of resynthesis of the TP. A degrader must ultimately overcome the homeostatic regulation of the target to suppress its levels, and this is more challenging

for proteins that have high rates of synthesis and clearance. Resynthesis rates vary quite widely for different proteins[10] (Alber and Suter – 2019) and some of the most therapeutically attractive targets are rapidly turned over in the cell. Compound properties, cellular (amount and concentration of E3 ligase) and TP dependent parameters, are critical and are collectively determinative for the modulation of the expected pharmacodynamic and ultimately therapeutic effect. A quantitative understanding of the onset rate and the extent and duration of the targeted pharmacologic effect (and additional secondary on-target effects) is key to determine the optimal combination of target protein and cell type, drug candidate and dosing regimen. In support of these TPD programs, pharmacokinetic/pharmacodynamic (PK/PD) modelling and simulation (M&S) has become an essential tool from the discovery phase to pre-clinical and clinical phases of drug development[11,12] (Tuntland et al. 2014, Grant et al. 2023). Despite glue degraders having physicochemical properties more associated with acceptable PK properties relative to the higher molecular weight and typically more lipophilic PROTACs, many challenges remain in the preclinical and clinical development of such novel TPD drugs. In particular, prolonged pharmacodynamic response is frequently observed following TPD treatment mainly due to nonlinear pharmacodynamic effects and toxicity caused by excessive target modulation[13] (Fang et al. - 2023). Low turnover rates of the targeted protein can further amplify this effect.

Most TPDs are currently directed towards oncological therapeutic targets. The mathematical modeling of tumour xenograft experiments following the dosing of antitumour drugs has received much attention in the last decade[14,15,16](Sardu et al 2015, Yates et al 2017, Simeoni et al 2004). Biomarker PD data can further provide useful insights on the pathological processes and be used for translational purposes in preclinical drug discovery and early clinical development. There is a paucity of published PK/PD models encompassing primary target modulation, additional secondary biomarkers of efficacy and/or toxicity and TGI. This work presents a global PK/PD approach for TPDs (figure 1) that can quantitatively relate primary target modulation to efficacy and be used for experimental data interpretation and simulation and for translating non-clinical efficacy data into human efficacious dose and regimen simulations via scaling of model parameters[15,17,18] (Yates et al 2017, Lignet et al. – 2023, FDA - 2023). For TPDs, it is of particular interest to develop integrated PK/PD models encompassing compound PK, TPD (as an essential biomarker of primary compound effect), secondary biomarker(s) connected to the cascade of events relating TP degradation to antiproliferative effect or to on-target side effects and tumour regression data as the safety/efficacy endpoint.

The approach described is aimed at establishing the reciprocal consistency of at least three types of models: compound vs PK, compound vs TPD (assumed as an indirect response model) and TPD vs TGI. An adoption of the residual TP as a translationally relevant biomarker can then be evaluated as already proposed in the biomarker-driven TGI models reported in literature[14,15] (Sardu et al 2015, Yates et al 2017).

For a TPD, using mathematical equations that separately describe the compound's effect on the target protein and the effect of target modulation on tumor growth inhibition allows us to simulate long TGI studies (6–8 weeks) based on degradation kinetics obtained from a much shorter (<1 week) in vivo experiment, provided the relationship between target modulation and TGI is already established.

Mathematical model generation allows the simulation of non-clinical and clinical biomarker and efficacy response with appropriate PK (predicted PK in the case of human) inputs. Directly estimating TP degradation via compound exposure implies the need to consider a cascade of events, especially if TP degradation is sustained in the absence of quantifiable circulating compound levels. A clear

advantage of our modeling approach is that it directly and quantitatively links TP degradation and resynthesis time dependency to efficacy or other on-target effects. Efficacy is indirectly linked to compound PK, facilitating the translation of effect to human, directly simulated and monitored via primary TP modulation (a parameter monitorable in the clinic typically via a liquid biomarker) and not exclusively based on compound exposure and clinical endpoints.

The modelling examples here reported have been taken from TPD programs in our company and are solely used to exemplify TPD modelling strategies. In particular, three case studies are presented exemplifying non-linear pharmacology associated complexities that modelling can help deconvolute, for example related to secondary efficacy biomarkers and to on-target hematological toxicities.

Methods

Theoretical

Our approach consisted of developing an integrated PKPD model encompassing compound, TP degradation and tumour-size data and not simply a compound concentration-driven tumour growth inhibition (TGI) model. Translating exposure to efficacy is then split in two key steps: 1) fitting compound dependent TP degradation and 2) quantitatively estimating TP modulation-efficacy dependency.

The tumour killing rate is related to the degradation of the TP, via the function f_{TGI}(TP), with the underlying assumption that the cell kill mechanism of action is strictly TP dependent with negligible off-target effects impacting the antiproliferative effect in the treated tumour cells. Indeed, undesired target protein promiscuity/degradation needs to be assessed throughout the duration of the drug discovery program. Selectivity challenges and considerations are beyond the scope of this article.

The PK/PD model consists of a PK component describing the plasma concentration compound profile with time (equation 1:1). It is assumed that plasma concentration may be used as a surrogate for tissue exposure and in particular the intra-tumoural unbound compound concentration is considered directly proportional to unbound plasma levels. Alternatively, plasma-tumour distribution model can be incorporated into the script, if experimental evidence supported its use, without altering the overall approach.

The second component of the PK/PD model (equations 1:2) details the TP degradation kinetics induced by the compound, an indirect response mechanism with compound induced stimulation of the degradation of response, where the response is the residual TP. An indirect PD model has been previously demonstrated to be consistent with the mechanism of action of PROTACs and monovalent degraders[19,20] (Guzzetti and Gutierrez 2023, J. Gabrielsson et al. 2018). In agreement with these publications, the Hill coefficient for monovalent degraders was set to 1.

The third component of this model is the equation relating the tumour size changes with time (equations 1:4, 1:5, 1:6, 1:7, 1:8). Equations 1:3 cover the modulation of biomarkers impacted by the primary target modulation.

For application in oncology discovery, this approach requires establishing a quantitative relationship between TP degradation and TGI effect. We adopted the Simeoni tumour growth model[16] (Simeoni et al. 2004) for the untreated tumour growth kinetics and assumed that the tumour killing rate due to a TPD is a mathematical function of the residual level of the TP.

The global system of differential equations used:

PK component describing the concentration compound profile with time:

$$\frac{dC}{dt} = \frac{In}{V} - \frac{CL}{V} * C \qquad 1:1$$

PD component describing TP degradation kinetics induced by the compound:

For monovalent degraders:

$$\frac{dTP}{dt} = k_{syn} - TP * k_{deg} * E_{max} * \left(1 + \frac{C}{DC_{50}+C}\right) \qquad 1:2a$$

For PROTACs, equation 1:2 can be generalized including the 'hook effect' in the model:

$\frac{dTP}{dt} = k_{syn} - TP * k_{deg} * \frac{1}{TPss}$; where TPss = 1- $D_{max} * \frac{C^h}{DC_{50}^h + C^h} * (1 - \frac{D_{loss}}{D_{max}} * \frac{C}{C + IC_{50}})$ 1:2b

the parameters in eq. 1:2b are detailed in Guzzetti and Gutierrez[19]

PD component describing biomarker modulation induced by TP degradation:

$\frac{dBIO}{dt} = k_{syn2} - BIO * k_{deg2} * (f_{BIO}(TP))$ 1:3a

or $\frac{dBIO}{dt} = k_{syn2} * (f_{BIO}(TP)) - BIO * k_{deg2}$ 1:3b

PD component relating the tumour size changes with time:

$\frac{dX1}{dt} = (\frac{\lambda 0 * X1}{[1+(\left(\frac{\lambda 0}{\lambda 1}\right)*TV)^{\varphi}]^{(1/\varphi)}}) - k_2 * f_{TGI}(TP) * X1$ 1:4

$\frac{dX2}{dt} = + k_2 * f_{TGI}(TP) * X1 - k_1 * X2$ 1:5

$\frac{dX3}{dt} = + k_1 * X2 - k_1 * X3$ 1:6

$\frac{dX4}{dt} = + k_1 * X3 - k_1 * X4$ 1:7

Tumour volume: *TV = X1 + X2 + X3 + X4* 1:8

Where C is the unbound TPD concentration in plasma; In, CL and V are, respectively, the input function of the TPD (for oral administration, normally the used input function is In = ka*A where A is the residual absorbable dose in the dosing compartment and ka is the absorption rate), unbound blood CL of TPD and its unbound volume of distribution. In this particular example, it is assumed a one-compartment model.

k_{syn} and k_{deg} are the zero-order TP synthesis rate and 1st-order TP degradation rate. In the absence of a TPD, the endogenous level of TP is constant: $TP_0 = k_{syn} / k_{deg}$.

In this model, the TP effect on the secondary biomarker is also indirect. Upon degradation of the TP, the biomarker level is modulated by modifying its rate of build-up or its rate of loss according to a function dependent of the residual level of TP: $f_{BIO}(TP)$). The choice could depend on the biological mechanism linking TP and the secondary biomarker. Similarly, k_{syn2} and k_{deg2} are the zero-order secondary biomarker (BIO) build-up rate and 1st-order secondary biomarker loss rate.

$\frac{dBIO}{dt}$ should be equal to zero at t=0; i.e. in absence of primary target modulation, when TP = TP_0.

Then applying eq. 1:3a,

$f_{BIO}(TP_0)$ must be = k_{syn2} / ($BIO_0 * k_{deg2}$) i.e. when TP = TP_0. eq. 1:3c

While using eq. 1:3b

$f_{BIO}(TP_0)$ must be = $BIO_0 * k_{deg2} / k_{syn2}$ i.e. when TP = TP_0. eq. 1:3d

More complex models could incorporate biomarkers like blood cells counts, to account for potential on-target, non-tissue specific dose-limiting toxicity, as reported by Abbiati et al. (Abbiati et al.- 2021)[21].

Often, the residual TP levels are expressed as fraction of the predose level TP_0. The eq 1:2 can then be replaced by eq. 1:2c:

$$\frac{dTP/TP_0}{dt} = k_{deg} - k_{deg} * \frac{TP}{TP_0} * (1 + \frac{C*E_{max}}{DC50+C}) \quad \text{1:2c}$$

Where TP/TP_0 is the residual TP fraction (TPf) remaining at time t. TPf is then equal to 1 at time zero (before any TPD administration).

An analogue simplification applies for eq. 1:2b.

This approach reduces the number of parameters to be determined by one as k_{syn}/ TP_0 is = k_{deg} but it does not allow the estimation of the absolute k_{syn} rate unless TP_0 is known.

For molecular glue degraders (i.e. in the absence of the hook effect), the lowest possible residual TPf, defined as the absolute Y_{min}, is the TPf at infinite compound concentration and, assuming the steady state is reached, (i.e. dTP/dt = 0), is equal to

TPf (C = infinite) = absolute $Y_{min} = 1/(1+E_{max})$ 1:2d

This means that E_{max} is related to absolute Y_{min} and vice versa.

Analogous to what was already achieved for compound-to-tumour and compound-to-biomarker models[14] (Sardu et al 2015), we can define the so-called TP degradation-to-tumour characteristic curve f_{TGI}(TPf) providing the asymptotic tumour size (TV) as a function of the steady state constant TPf level (i.e. assuming the TPD is constantly infused in the xenografted animals for an infinite time in order to reach a constant steady level of TPf).

Assuming a steady state (ss) is achieved, if the tumour size TV is < ג1/ג0 (where ג1/ג0 = critical tumour volume), equation 1:4 can be approximated to:

dX1/dt = ג0 $*X1$ – k_2*f_{TGI}(TPf)* $X1$ = $X1$ *(ג0 - k_2*f_{TGI}(TPf)) (1:4b)

Which becomes negative (= tumour regression) when f_{TGI}(TPf) > ג0/k_2 (1:4c)

Then dX1/dt = 0 if $X1$ is 0 which means that $X1$ is asymptotically stable only at complete tumour regression.

Conversely, if f_{TGI}(TPf) < ג0/k_2, the tumour growth will be only slowed down reaching a final steady state size:

Assuming TV>ג1/ג0, it implies that eq 1:4 can be approximated to dX1/dt = ג1 $*X1$/TV – k_2*f_{TGI}(TP)* $X1$ (where TV = X1+X2+X3+X4) (1:4d)

At ss dX2/dt = k_2*f_{TGI}(TPf)* $X1$ – k_1* $X2$=0 and (1:4e)

dX3/dt = k1*(X2-X3) = 0 and dX4/dt = k1*(X3-X4) = 0 (1:4f)

as a consequence: X2 = (k2/k1)*$X1$ * f_{TGI}(TPf) = X3 = X4 (1:4g)

dX1/dt = ג1 $*X1$/TV – k_2*f_{TGI}(TPf)*$X1$ and then

$$X1 = \frac{ג1}{1+3*(k_2/k_1)*f_{TGI}(TPf))*k_2*f_{TGI}(TPf))} \quad \text{(1:4h)}$$

and TV at steady state (TV(ss)) = $X1$ * (1+3∗(k_2/k_1)∗ f_{TGI}(TPf)) (1:4i)

which implies that TV(ss) = ג1/ (k_2*f_{TGI}(TPf)) > ג1/ג0 (i.e. > critical TV).

Finally, If f_{TGI}(TPf) = ג0/k_2 (1:4l)

ג0 ∗ $X1$ – k_2* f_{TGI}(TPf) ∗ $X1$ = ג0 ∗ $X1$ – k_2* ג0/k_2 ∗ $X1$ then $X1$ is indefinite with a value

$$0 \le X1 \le \frac{ג1}{ג0 * (1+3*(ג0/k1))} \quad (1:4m)$$

By determining the tumour parameters and identifying the relationship (k_2*f_{TGI}(TPf)) between the residual TP fraction in tumour cells and the resultant tumour killing rate it is possible to identify the threshold TPf value required to achieve tumour stasis.

One of the distinct advantages of this approach, is that assuming that the TGI is strictly related to TP degradation (i.e. that two compounds yielding the same TP degradation profile will produce the same TGI, independently of their potency and PK), a simulation of tumour cell killing of a new TPD in a xenograft model can be performed by determining the k_{deg}, Emax and DC50 *in vitro* and *in vivo* PK parameters, facilitating optimal study design with ethical, time and cost savings advantages.

Case studies specific equations:

Case study A: model estimated TPf value achieving at least tumor stasis

For case study A, TPf estimation for tumours regression in CDX1 and CDX2, was based on

eq 1:4c and 1:4l : f_{TGI}(TPf) ≥ ג0/k_2.

Where = f_{TGI}(TPf)) = (1/(TPf)-1)^ϒ (2:2d)

Then TPf ≤ 1 / (1+ (ג0/k_2)^(1/ϒ) (2:2e)

Case study B: biomarker modulation induced by TP degradation

For the secondary biomarker, the adopted equation was 1:3a, where:

$f_{BIO}(TP)$ = $Emax_2$ * (TPf)^Gam_2 / ($EC50_2$^Gam_2 + (TPf)^Gam_2). (3:1)

When TP = TP_0, TPf =1, BIO_0 =1 (expressed as relative fraction respect to when no treatment is applied) then, according to equation 1:3c :

k_{syn2}/k_{deg2} = $f_{BIO}(TP_0)$ = 1+ $Emax_2$/($EC50_2$^Gam_2+1). (3:2)

To note that according to the form of the equation written in the model, a negative gamma value is obtained following parameters estimation, indeed as the TP is degraded, the secondary biomarker loss rate is also increased, then the term (TPf)^Gam_2 / ($EC50_2$^Gam_2 + (TPf)^Gam_2) shall increase as TPf decreases.

According to the model parameters estimated from the experimental data,

1+$Emax_2$/($EC50_2$^Gam_2+1) is approximately = 1

as the second term in the equation above is negligible respect to 1, then also in this case, k_{syn2} can be assumed with good approximation equal to k_{deg2}.

Case study C: biomarker modulation induced by TP degradation

For the secondary biomarker, the adopted equation was then 1:3b, where:

$f_{BIO}(TP)$ = (1 / (TPf^φ)) (3:4)

The choice of these equations was informed from i) the observation of the experimental data and ii) the biologic mechanism of action, suggesting that the degradation of the TP stimulates the biomarker synthesis, but alternative options (i.e. using equation 1:3a where $f_{BIO}(TP)$ = (TPf^φ)) could be mathematically equivalent as the ratio: rate of synthesis/rate of degradation calculated for the biomarker would be the same using the two approaches.

Clearly when TP = TP_0, TPf =1 and $f_{BIO}(TP)$ = 1, BIO_0 is also equal to 1 (if expressed as relative fraction respect to the untreated case) then k_{syn2}=k_{deg2} to respect the general eq 1:3c and 1:3d.

Experimental

Xenograft studies.

Human derived tumour cells (usually 1-5 x 10^6 cells/animal 1:1 in matrigel) were implanted into the flank of nude or severe combined immune-deficient mice and tumours allowed to grow. Once tumours had reached a predefined size (100–300 mm^3), mice were randomized to different treatment groups including a vehicle control group.

Tumour volumes determined before the initiation of treatment were considered as the starting volumes[22] (Alard et al. 2023).

In all these examples, the compound was administered with *quaque die* (qd) or *bis in die* (bid). oral (po) bolus dose to female mice (usually n = 12/dose). When bid, the second daily dose was administered 8h after the first dose. Dosing volume was limited to 5mL/kg per administration.

For preliminary target degradation PK/PD investigations (used to estimate PK parameters and k_{deg}, DC_{50} and E_{max}), animals were treated with a single dose or with repeated administrations (typically for 3 to 7 consecutive days). After the last administration, normally 4 animals per time point were sacrificed, compound concentration was measured in plasma and tumour tissue, while target degradation was measured in tumour tissue only. Tumour size was typically not considered as a relevant endpoint in these short-term studies. When applicable, eventual biomarkers were measured in tumour tissues.

For efficacy investigations, animals were treated with repeated administrations for several weeks, depending on tumour growth rate in the untreated (vehicle) group. Tumour size was recorded at least twice a week in all animals, across all groups. After the last administration, 4 animals per time point were sacrificed, compound concentration was measured in blood and tumour tissues while target degradation and other eventual biomarkers were measured in tumour tissues.

The Evotec Ethical Committee — accredited by the International Association for Assessment and Accreditation of Laboratory Animal Care (AAALAC)—reviewed all the in-life study plans to assess the compliance with the corresponding authorized project as defined in Directive 2010/63/EU.

Efficacy was determined as $\%TGI = (1-\{T_t/T_0 \,/\, C_t/C_0\} \,/\, 1-\{C_0/C_t\}) \times 100$ where T_t = median tumor volume of treated at time t, T_0 = median tumor volume of treated at time 0, C_t = median tumor volume of control at time t and C_0 = median tumor volume of control at time 0.

Compound concentrations in plasma and tumour were determined by LC/MS-MS. Unbound compound concentrations were estimated from plasma protein bound fraction and tissue homogenate bound fraction, measured in vitro in separated experiments. Target protein level in tumours and secondary PD biomarkers were measured using MesoScale technology or Western-blot analysis.

In all the case studies here presented, unbound plasma concentration was used for the PK/PD equations in the model (estimated from the total plasma concentration, corrected by the plasma protein binding[19,23], (Waters et al. 2008). Tumour total and unbound concentration (estimated from the total tumour concentration, corrected by the protein binding to tumour tissue homogenate) were used to verify if the TPD partitioning between tumour and blood was rapid enough to assume achieved steady state at the time of sampling and if plasma and tumour unbound concentrations were comparable. As tested compounds were optimized to have rapid passive permeability, measured tumour unbound compound concentrations were always in good approximation comparable to the corresponding unbound compound concentrations in plasma. This resulted in no requirement to

model compound distribution from the systemic compartment to the effector (tumour) compartment[20,24]. (Gabrielsson et al. - 2018, Zhang et al. - 2019).

PK/PD modelling and simulations

PK and PD parameters were derived using Phoenix WinNonlin (version 8.3.5, Pharsight Corporation as part of Certara, St. Louis, MO).

Experimental values used as input data were the average values measured from all the animals sampled at each time point, per each dose group. Parameters estimations were executed using the naïve pooled algorithm and assumed identical in all treated groups.

In occasion of the TGI *in vivo* experiments, adopting the standard study design described above, the number of collected time-points post last administration for PK and target protein degradation analysis, was often limited to four. This is a limited dataset and to let the software determine all the parameters in the xenograft efficacy model, parametrization was in general performed in three steps. Step 1: the data from the single and repeated dose PK studies in mouse were pooled to fit a mouse PK model. Step 2: the TPf data from the single and repeated dose PK/PD studies were pooled to fit a PD model, using plasma concentrations simulated with the PK model parameters estimated in the previous step (i.e. "freezing" the PK parameters previously optimized in step 1). Step 3: the tumour proliferation parameters, including the ones in the f_{TGI}(TPf) expression of the model, were estimated by fitting the experimentally measured tumour volume values and simulating the residual TPf modulation at the doses used in the TGI study, "freezing" the parameters estimated in the steps 1 and 2.

Results and Discussion

Study case A:

Study Case A describes how to quantitatively relate degradation of the TP to tumour cell kill rate and, as a cumulated effect with time, to efficacy.

The TP (Protein A) is considered a novel cancer therapeutic target, and Compounds 1, 2 and 3, act as molecular glue degraders of the TP. These compounds were characterised by time dependent decrease of the TP degradation Y_{min} value in the in vitro cellular assay (data not shown). All compounds demonstrated good passive permeability, with low to moderate clearance in mouse. The oral plasma profile of these compounds in mice followed a single compartment PK, with first order absorption rate and dose proportional clearance.

The PKPD model made the following assumptions, applicable to all 3 compounds, that were validated against the data:

1. PK in mouse is linear.

2. Plasma unbound concentration may be used as a surrogate for tumour unbound concentration. K_{puu} plasma/tumour values were close to unity and comparable at all sampled time point, with no apparent time dependency.

3. Degradation of TP is directly correlated with tumour growth inhibition. That is, tumour killing rate is a function or the residual level of the TP f_{TGI}(TPf)); this is a foundational assumption for all tumour killing TPD projects and is within the mathematical PKPD model yet needs to be verified with experimental data.

Figure 2 shows a correlation between the residual Protein A determined in tumours for each tested dose of compounds 1 and 2 (reported value is the average of all the time points collected within the dose interval) and the relative TGI% value measured at the end of the study. Compounds 1 and 2 demonstrated partial (growth inhibition) and extensive (tumour regression) in vivo efficacy respectively. Collected data support the assumed MoA, as there exists a strong inverse proportionality between tumour growth rate and fraction of TP degradation.

The plot also shows two proposed fitting curves described by equation 2:2a and equation 2:2b respectively.

$$TGI\% = (1/(TPf)-1)^{\gamma} \quad (2:2a)$$

$$TGI\% = (1-TPf)^{\gamma} \quad (2:2b)$$

These equations relate the final TGI% value to the average TPf value experimentally determined. The TGI effect cumulates with time from the start of treatment and according to dosing regimen. The killing rate is instead mathematically related to instantaneous TPf value; still, a similar relationship between the function f_{TGI}(TPf)) in equation 1:4 and TPf was assumed.

$$f_{TGI}(TPf)) = (1/(TPf)-1)^{\gamma} \quad (2:2c)$$

Alternatively, the second explored form for f_{TGI}(TPf) function is described by eq. 2:2d

$$f_{TGI}(TPf)) = (1-TPf)^{\gamma} \quad (2:2d)$$

The parameter gamma in both 2:2c and 2:2d defines the shape and the steepness of the relationship between TP reduction and cell kill rate.

Equation 2:2c describes an increasing cytotoxicity with an infinite killing rate achieved as the residual TPf approaches zero whereas equation 2:2d describes the killing rate reaching a maximum value as the TPf approaches zero.

Figure 3 shows the dependency of the proposed functions 2:2c and 2:2d vs gamma as the residual level of TPf changes. Both equations proved to be quite efficient in modelling the TGI data collected during this case study when they were directly compared (data not shown), with neither of the two equations evidently superior.

As TPf can only reach the lowest value of $1/(1+E_{max})$ (eq 1:2d) it is often challenging to extrapolate the f_{TGI}(TPf)) curve profile at TPf tending to zero, which remains an intrinsic experimental limitation. This explains why two different curves like 2:2c and 2:2d may both adequately fit the data when the experimental TPf remains significantly above zero.

One merit of applying both equations is to demonstrate good fitting of the experimental data by using a single parameter, minimizing the risk of excessive parametrization and poor identifiability of the model. -figure 4 demonstrates how the PK/PD model fit the experimental tumour volumes obtained by degrading the TP A. (figure 4A for compound 2 in CDX 1). In this experiment, the high dose group was not immediately sacrificed after the end of the dosing period (744 h) but was kept untreated for additional 600h to observe the tumour regrowth profile which was indeed observed and adequately fitted by the model.

Figure 4B shows the fit of data for compound 3 tested in CDX 2, and also shows a good agreement between experimental and simulated values. For two different compounds and CDXs, the same mathematical approach was successfully applied. In these specific examples, the f_{TGI}(TPf) function

2:2c was used. Equation 2:2c was also used for different programs (case studies B and C), proving to be fully adequate at modelling different targets degradation-tumour kill rate relationships.

The good visual fit was also confirmed by the strong correlation (figure 5) between all the simulated and the experimental observables testing compound 2 in CDX1 (compound concentration, TPf and tumour size). Similar good fits were also obtained for compound 3 in CDX2. The fit of the model to the experimental data in figure 4 allowed us to consider the model validated for further use.

A key question the model was applied to answer was how low the TP A is required to be degraded to achieve a minimally desired endpoint, e.g. tumour stasis. This value is of primary importance because its use for translational purposes will contribute in defining the estimated minimal effective dose in human and consequently the derived therapeutic index.

Equations from 1:4b to 1:4m demonstrated how by determining the tumour parameters and identifying the relationship ($k_2 * f_{TGI}$(TPf)) between the residual TP fraction in tumour cells and the resultant tumour killing rate it is possible to identify the threshold TPf value required to achieve tumour stasis. The tumour growth and the f_{TGI}(TPf) estimated parameters are reported in table 1 in both CDX 1 and CDX 2 (fig 4). These inferred values were used to calculate the residual TPf that led to tumour stasis according to eq. 1:4l and eq. 2:2d and 2:2e (for additional details relative to the equations adopted in the model refer to the "Case studies specific equations" of the Theoretical methods section). These values correspond to 20% for CDX 1 and 16% for CDX 2. For CDX1, the achievable Y_{min} is 18% showing that tumor regression is attainable, also according to the model. For CDX 2, estimated E_{max} = 4.3 suggests a Y_{min}% of 19% while the other model parameters indicate a minimum of 16% (TPf = 0.156) for tumour regression, explaining why even at the top tested dose, we only observe partial tumour growth inhibition and not stasis or regression. Tumour cell kill in additional CDXs and PDXs was investigated via the same TP degradation mechanism. Figure 6 demonstrates TGI resulting from Compounds 1, 2 and 3 tested at multiple doses, in 3 different CDXs plotted against TPf (the average TPf values across the different time points tested). Each condition tested, i.e. each compound, dose level, TPD and CDX combination, represents an individual data point in the plot. Figure 6 has been adapted with respect to figure 2 to better visualize TPf values reaching tumour stasis. Among the different tested xenografts, the overall trend shows a comparable dependency of TGI from the remaining TPf, suggesting that reduced residual TP levels are, in a similar way, progressively blocking the cell proliferation rate among different tumour types. This evidence further confirms the applicability of equations 2:2 to additional tumour cell lines.

Consistent with the PK/PD model, the same compound and dose achieved different TPD levels in different tumour cell lines, despite equivalent PK in mice, demonstrating efficacy was strongly and better correlating with the residual level of the TP and not compound exposure *per se*. The achievable Y_{min} of the targeted protein can be cell dependent. Sobierajski et al. 2024, reported that the expression levels of known E3 ligases vary depending on the cell type, subcellular localization, cell cycle, and species studied.[25] Different CDXs may then require different TPD compound exposure, even for the same tested compound, to reach the targeted efficacy endpoint (expressed as tumour growth inhibition %).

Despite similar residual TP levels driving similar antiproliferative effects in different mouse xenograft models, according to our PK/PD analysis, faster proliferating tumours may require deeper TP degradation. The lowest TPf value estimated by our modelling approach, in one of the most difficult to treat CDX, (indicated as TPf = 0.156 in figure 6) split all the datapoints in two main clusters, separating conditions achieving tumour regression from partial proliferation inhibition. This TPf threshold value

resulted in efficacy in both the most and least responsive tumour types tested, including PDXs, and was thus applied as a translationally relevant target value in human.

For translational PKPD purposes, human PK parameters were predicted following well-established methodologies using human in vitro and animal PK data (details not showed) (Grime et al. - 2013)[26], (Davies et al. – 2020)[27], (Lombardo et al. 2016) [28], (Fonsi et al. - 2008)[29] Human PD parameters related to TP degradation were estimated from non-human primate (NHP) PK/PD studies based on the following rationale and results. The collected data are shown in table 1. The purpose is to exemplify the types of data required to be generated to be considered for use in a translational PKPD modelling strategy.

In vitro TP degradation was observed in human and NHP blood cells (whole blood cells and PBMCs) with DC_{50} and Y_{min} respectively, yet only at high concentration in rat and not at all in dog and mouse (data not shown). Likewise in vivo, degradation was observed in NHP healthy tissues, including blood, but not in mice and dogs and only at high dose in rats. TPf values in NHP blood agreed with TPf values in other tissues collected ex vivo (Y_{min}% = 3% in PBMCs; 10% in colon; 3% in liver; 3% in kidney; 2% in lungs). In addition, for NHP, in vivo degradation measured in blood cells were consistent with in vitro results. For NHP, in vivo blood TP degradation kinetic parameters (k_{syn}, k_{deg}) were comparable to values measured in tumours CDXs (see table 1) providing confidence in applying these values for translational use to human, whilst DC_{50} and Y_{min} were estimated from human in vitro blood cells and found comparable to NHP in vitro (D50s = 0.5 nM and 0.6 nM in human and NHP respectively; averages of n=6 donors/species) and in vivo (NHP D50u = 0.6 nM and 2.3 nM in vitro and in vivo respectively - see table 1). Thus, blood cells derived data can be considered a valid in vivo biomarker of TP degradation, both for non-clinical and future clinical PD/safety investigations. Rat and NHP were adopted as safety species

The lowest effective dose in human was simulated using the predicted PK and PD parameters as described above and by targeting the averaged residual level of TP assuring tumour stasis as minimal efficacy, as described in figure 6 and according to equation 1:2a.

Study case B:

Study case B describes a different pharmacological TP in oncology. According to the known biological pathway, the TP degradation is associated with the decrease of a secondary biomarker previously related with tumour cell kill.

Molecular glue compounds were initially investigated in vitro and, the most promising ones such as compound 6, also in vivo in xenografted mice (CDX4) assessing TP degradation, secondary biomarker modulation and antiproliferative effects. In vitro and in vivo investigations used the same tumour cell type.

Initial in vitro investigation showed the TP degradation reaching a steady state Y_{min} value within 24h while for the secondary biomarker, a steady state was only achieved after more than 65h. In vivo PK/PD studies in female NXG mice demonstrated that the initially adopted 3 days BID regimen was insufficient to reduce secondary biomarker levels to the values observed in vitro, consequently dosing was extended to 7 days, showing further biomarker loss on day 7. This data confirmed the primary target-secondary biomarker relationship to be strongly time dependent. Equation 1:3a was included in the model to simulate the data.

Figure 7 shows the experimentally determined relationship between the residual fraction of the primary TP and the relative modulation (treated group vs control vehicle group) of the monitored secondary biomarker as consequence of primary TP modulation. The plot includes in vitro and in vivo data and demonstrates i) a strong in vitro-in vivo concordance and ii) a sigmoid relationship between primary TPf and the secondary biomarker residual values. A line was fitted using a classic sigmoid relationship BIO = E0 + $Emax_2$ * (TPf)^Gam_2 / ($EC50_2$^Gam_2 + (TPf)^Gam_2) (eq. 3.3 - Table 2).

$EC50_2$ represents the TPf value giving 50% of the maximum biomarker modulation, E0 is the relative secondary biomarker fraction when the TPf goes to zero (even if the minimum level of TPf achievable with a molecular glue compound is limited to the corresponding Y_{min} value), $Emax_2$ is the maximum achievable secondary biomarker reduction via TPf degradation and Gam_2 is the Hill coefficient of the sigmoid curve.

The data in the plot in figure 7 were determined after 7 days of in vivo treatment or 96h of in vitro incubation of Compound 6; it was assumed pseudo-steady state was achieved in both cases. Nevertheless, an analogue equation (eq. 3:1) was used in the model to predict the indirect response to the target degradation, elicited in term of biomarker loss-rate change.

The global in vivo model adopted was based on the same assumptions described for case study A, except for the non-linear PK, i.e. unbound compound concentration in blood was assumed proportional to unbound compound concentration at the target compartment, due to constant plasma/tumour concentration ratios at each sampling time point. The secondary biomarker levels were linked to the degradation of the TP via equation 1:3a, where $f_{BIO}(TP)$ form is defined by eq. 3:1 and eq. 3:2. Finally, the degradation of the TP was directly correlated with tumour growth inhibition using eq. 2:2c. (for additional details relative to the equations adopted in the model refer to the "Case studies specific equations" in the Theoretical methods section).

The comparison between measured and simulated secondary biomarker levels is reported in figure 8. Figure 8b shows the time required for biomarker modulation; the time to reach a steady state level for the secondary biomarker is predicted by the model to be dose dependent becoming shorter as the dose increases. Analyzing the data with the fitted simulation exemplifies the utility of applying modeling and simulation early in TPD drug discovery.

Figure 9 shows the concordance between measured and model fitted tumour volumes upon dosing compound 6 at three different doses in *in vivo* mouse model CDX4. Model parameters simulate tumor stasis in CDX4 when the TPf is 0.04 (eq. 2:2 d and 2:2e); while the model estimated Y_{min} is 0.034 (Y_{min} % = 3.4% – see details in table 3a). The absolute Y_{min} is quite close but still lower than the estimated value for tumour stasis, then, according to the model, tumor regression is still possible upon achieving adequate compound exposure, as demonstrated at the high dose. In this experiment, the high dose is 10-fold higher than the low dose level, with a more than dose proportional increase in exposure (see Fig. 9b); the corresponding observed increase in TGI% goes from 75% to 114%. This relatively flat dose response is understandable by the expected non-linear TPf-concentration relationship for TPDs (eq. 1:2a) and the maximum degradation achievable by this compound (Y_{min}) which, for this CDX, is approximal to the TPf value simulating tumour stasis.

Figure 10 plots the secondary biomarker modulation vs. TGI after 38 days of treatment. The observed linear fit compares very well with previous data using different antitumoral molecules and different CDX models (data not shown). Secondary biomarker modulation following TP degradation can be more rapidly investigated with a 7-days PK/PD study and modeled including a quantitative relationship between TP degradation and the validated secondary biomarker of efficacy (the simplified PK/PD model is shown in fig. 11). A shorter PK/PD experiment can then be used to parametrize drug

dependent secondary biomarker modulation and used to anticipate the outcomes of TGI experiments (as in figure 10) normally lasting more than one month and requiring a larger cohort of animals. This case example demonstrates the value of such an approach to compounds selection in TPD drug discovery.

Tables 3a and 3b show the overall In vitro and in vivo PD parameters comparison for compound 6 in CDX4 and in PBMCs.

For the tumour cell line used in CDX4, in vitro and in vivo in mice DC_{50} and Y_{min} values were comparable (Table 3a), showing good in vitro-in vivo correlation, then confirming the robustness of the in vitro screening approach for in vivo target degradation (and efficacy). Based on this, it may be anticipated that the in vitro proliferation assay using patient derived tumor cells may also offer reliable indications for selecting responsive cancer genotypes to be further confirmed in PDX in vivo models.

Comparing DC50, Y_{min} and $k_{syn}/[TP_0]$ values obtained in vivo, in human derived tumor cells implanted in mice (CDX4) and in PBMCs from non-tumor bearing animals (table 3a), we observe a general consistency among the values. PBMCs investigated in vitro demonstrated strong TP degradation in human, rat, dog and NHP. Dog, human and NHP DC50 and Y_{min} values were closely comparable (table 3b).

Close evaluation of the therapeutic index of the target/drug candidate in preclinical species is critical before candidate nomination. Based on the PK/PD and efficacy analysis conducted in the CDX4 model, we may expect to observe efficacy in patients when the residual TPf drops below 0.04. *In vivo* preliminary safety assessment was carried out in rats and dogs and aimed at investigating potential drug and target-related safety issues, thus achieving adequate drug exposure and target engagement in the selected species, comparable to humans at effective doses[30], was necessary. The TPf measured in rat and dog, in PBMCs and tissues, are reported in table 4. These data, even if preliminary, show achievable target engagement in safety species, in the range of expected efficacy in human. The low dose in dog was chosen as approximately equivalent to the human expected dose targeting an average TPf ≤ 0.04 (i.e. ≥96% of target degradation), according to a model simulation based on eq. 1:2a, 1:2d and on initial in vivo PK/PD data in dog (table 3a). TPf in PBMCs and the average data in tissues experimentally confirmed the preliminary model simulation. Overall, these results suggest that PBMCs can well recapitulate target degradation in tissues and supported as liquid biomarker in preclinical and clinical phases for both efficacy and safety, then used to estimate the therapeutic index of the drug candidate and of the target.

TPDs can be effective without requiring large excesses of circulating compound due to their catalytic mechanism. Estimating target-related effects via compound exposure may become less informative and inadequate for representing PD time dependency. Case study B can be used as a reference example with a delay before achieving steady state in the modulation of the secondary biomarker, as well as an interval after the end of compound administration to restore initial physiologic levels. Both primary and secondary biomarkers demonstrated no parallel time dependency with compound at steady state. Delayed PD effects may include toxicity induced by on-target, non-tissue-specific effects31 (Cheng et al. - 2024). Abbiati et al.[21] focused their model on neutropenia yet did not integrate with an efficacy-PD model for tumour suppression, adopting compound exposure as a surrogate endpoint for efficacy, assuming direct proportionality between exposure and efficacy. However, for all these case studies, we have demonstrated the intrinsic non-linear PD behavior for TPD which needs to be incorporated to more accurately simulate doses and dosing schedules that use dosing holidays to achieve efficacious exposures while maintaining tolerability from on-target protein degradation.

The good IVIVC observed between TP degradation and secondary biomarker modulation confirmed the predictivity of *in vitro* PD models which have been used for drug candidate selection and optimal compound design as well as for translational purposes. The preexisting data relating secondary biomarker modulation to efficacy in several CDX models, confirmed also by our in-house data, can be used to anticipate efficacy from shorter PK/PD experiments compared to full TGI assessments.

Study case C:

The TP in this study case is also a novel anticancer protein targeted via use of a molecular glue degrader. Based on the biological pathway, the TP is involved in cell proliferation, yet its function is believed nonessential for viability. Its degradation is associated with the increase of a secondary phosphorylated protein which is hypothesised to directly correlate with an antiproliferation effect.

The PK/PD model was extended to quantitatively relate the degree of TP degradation to a secondary biomarker modulation, assumed potentially prognostic of efficacy. After initial screening in vitro, compounds were tested in vivo in CDX5 with plasma and tumour samples collected at different time points post dose after the last of 7 days b.i.d. administrations. Samples were analysed for PK (plasma and tumour) and PD (tumour) investigations.

The PK/PD model was based on similar assumptions described for case study A and B. For the secondary biomarker eq. 1:3b was adopted. To anticipate the best mathematical form for the generic function $f_{BIO}(TP)$, the experimental data were inspected. Figure 12 shows the relationship between the residual fraction of the TP and the relative fold increase of the secondary biomarker (treated group *vs*. control vehicle group) as a consequence of TP modulation for two different compounds (compounds 4 and 5) in CDX5. In the same plot, a line was fitted using the empirical relationship BIO = 1 / (TPf^φ).

Similar to case study B, figure 12 plots data collected at different doses, but also at different time points during the study and we expect the TP-biomarker relationship to be time-dependent. This is according to the model hypothesis that the TP degradation impacts the rate of synthesis of the secondary biomarker and not directly (instantly) the expression level, with a consequent indirect effect with time. An analogue equation was used in the model to simulate the indirect response to the target degradation, elicited in term of biomarker production rate modulation: $f_{BIO}(TP)$.

Equation 3:4 was used for $f_{BIO}(TP)$, as explained in the Theoretical Methods section.

Plotting the simulated level of the secondary biomarker with time (figure 13), we obtain an overall good fit with all experimental data except for 3 points, suspected to be potential outliers. This finding advised a further analysis of initial input data: the absolute residual differences between the values predicted using the equation BIO = 1 / (TPf^φ) above and the experimentally measured values, were plotted using the interquartile range plot analysis (inlet plot in figure12). Data circled in red are then identified as probable outliers, based on Tukey box plot analysis[32].

Beyond confirming that the TP degradation is associated with the increase of the secondary phosphorylated protein, adopted as secondary biomarker of efficacy, this quantitative correlation suggested the indirect link equation form between target degradation and protein phosphorylation.

In the model, tumour growth inhibition was directly correlated with degradation of the TP using eq. 2:2c. Compound 5 was administered *b.i.d* for several weeks in CDX5 and tumour volumes were measured and compared to vehicle group. Figure 14 shows the relationship between simulated and

measured tumour volume. The visual inspection of simulated and measured values confirms the accuracy of simulations and the adequacy of the mathematical form given to the adopted model equations.

We have already discussed for case study B the translational relevance of estimating the therapeutic index of the candidate and target combination via in vitro data and in vivo in relevant species. As reported in Table 5, Human (CD34+), NHP and dog bone marrow progenitor cells were exposed in vitro to compound 5 showing sub-nanomolar cytotoxicity against dog and human myeloid (IC50 = 0.13 and 0.15 nM in dog and human respectively) and erythroid lineages (IC50 = 0.18 and 0.19 nM in dog and human respectively) but a significantly higher IC_{50} was measured in NHP cells (IC50 values ranged between 21 and 37 nM). Rodent myeloid and erythroid lineages were instead relatively insensitive (IC50s values were >700nM). Hematologic findings were attributed to on-target effect due to the comparable in vitro values for DC_{50} and IC_{50}. In addition, i*n vitro* data also showed regenerative capacity for both myeloid and erythroid cells once the compound was removed from the incubation with capacity for cells to continue proliferating. These observations suggested that intermittent dosing schedules could be explored to improve the therapeutic index and the PKPD model used to simulate the TGI effect of different dosing regimens in the design of preclinical efficacy studies. Likewise in vivo hematology data would be informative during the preclinical safety assessment and before FIH.

Based on target degradation in PBMCs, in vivo PK/PD data in NHP also showed higher Y_{min} values compared to dog (24% and 0.5% in NHP and dog, respectively). While DC_{50} in dog PBMCs is 10 times higher than in human, in vivo Y_{min} and $k_{syn}/[TP_0]$ values measured in dogs and in CDX tumors were closely comparable (Table 5). As a consequence, dog was considered a more appropriate animal model for translation both in terms of efficacy and safety.

At the time of writing, no hematologic in vivo data are available. Once data will be available, an adequate PK/PD model able to describe target modulation dependent efficacy and toxicity can be used to anticipate the potential therapeutic benefit *versus* the risk of hematic toxicity in human and as an input to the monitoring of the tolerability of this novel therapeutic intervention during the initial exploration of different clinical doses and dosing regimens.

Conclusions

Targeted protein degraders (TPDs) are a promising class of anti-cancer drugs. Optimal design of TPDs requires a mechanistic understanding of efficacy and toxicity drivers (Fig 1). This manuscript provides a translational PK/PD framework based on real case studies in drug discovery. A general PK/PD model structure for anticancer protein degraders is proposed. The goal in TPD drug discovery is to deploy a quantitative modelling that describes the relationship between target degradation and tumor growth inhibition, that also identifies excessive pharmacodynamic response that may cause on-target toxicity. Input from PKPD modelers into in vitro and in vivo study design, analysis, and interpretation can elucidate the relationship between PK and PD, enhancing the translation of in vitro compound potency to in vivo settings and identifying key properties for optimal TPD design.

Fit-for-scope preclinical in vivo studies are crucial to understand the therapeutic potential of new targets or drug candidates and confirm in vitro-in vivo correlations (IVIVC). A global PK/PD approach is indispensable for modeling complex processes like TPD-induced protein degradation and its quantitative relation to efficacy. Predictive PK/PD models require mathematical descriptions and parameterization based on available datasets. Equations should be consistent with cellular mechanisms, translating degrader pharmacology into mathematical language to identify responding tumor cells.

The three case studies presented herein demonstrate the utility of PKPD in TPD drug discovery. Quantitative relationships between primary targeted protein modulation and efficacy endpoints can be extrapolated using experimental PD data. Drug discovery teams face hurdles such as limited knowledge of novel targets' impact on tumor cell growth and low sample throughput, this results in low statistical power in discerning generalizable patterns from cohort-specific effects. In addition, non-robustness and irreproducibility of sample preparation and the analytical setups may result in high analytical variability[33] (Jakob et al. - 2023). Careful analysis of input data is critical for successful model parameterization. Data from testing prototype tool compounds (that may not have all associated properties optimized for candidate drugs) during early drug discovery can enrich datasets and accelerate drug candidate optimization and selection. Moreover, as exemplified for the case studies A, B and C, PK/PD modeling enables quantitative translational hypotheses to be formed from in vivo animal and in vitro human data to the clinic.

Case study A describes how to quantitatively relate degradation of the TP to tumour cell kill rate and, as a cumulated effect with time, to efficacy. Case studies B and C demonstrate how secondary biomarker data can simulate tumor growth inhibition (TGI) efficacy from simpler PK/PD studies, saving time, resources, and reducing animal use. Mathematical equations were used to model secondary biomarker modulation as a function of TP residual fraction. Key model parameters like DC50, Y_{min}, and target protein resynthesis rate were extrapolated using PDX models and blood-derived biomarkers and incorporated into translational simulations for human. Human PK parameters, required to simulate the impact of clinical dose and dose regimens can be predicted by well-established methodologies for drug candidates[27] (Davies et al – 2020) but were not the focus of this report.

A minimal human efficacious dose and regimen can be estimated by simulating a targeting of stable disease (tumor stasis). It is recognized that tumour doubling time is slower in patients than in xenograft mouse models, thus the approach presented here may be conservative and this difference can be incorporated into the model by scaling allometrically tumour growth parameters[34,35] (Tosca et al. 2024; Betts et al. 2020). Likewise, simulations that achieve stable disease based on such translational PK/PD benchmarks (as presented here) can be assumed to be only minimally efficacious in humans, and of

course the targeted effect is to achieve tumor regression for a clinically meaningful proportion of patients (Betts et al. - 2020)[35]. PKPD modelling approaches may elucidate drug dosing regimens for both efficacy and tolerability, improving the clinical exploration of the optimum therapeutic index for TPDs. A similar model to the one here presented for on-target effects can consider off-target modulation, with minor modifications.

In conclusion, we have presented a mechanism-based PK/PD modelling framework, not only characterizing the disposition of TPDs and TP degradation but also providing a translational framework of non-clinical PD, efficacy and indeed on-target toxicity data to the clinic. The methods described do not directly translate exposure into efficacy but deconvolute protein degrader effect by separating the PK/PD model in two key steps: 1) modelling of compound dependent target protein degradation and 2) quantitatively estimating TP modulation-efficacy/effect dependency thus quantitatively describing and simulating desired and undesired effects directly related to primary target modulation. This mathematical framework results in positive impacts in both experimental design and compound optimization in drug discovery and a more quantitative and ultimately predictive set of translational tools.

Special thanks:

We acknowledge the contribution of our colleague, Xavier Boulenc, who peer reviewed the PKPD model and offered helpful suggestions.

References

[1] Dang CV, Reddy EP, Shokat KM, Soucek L. Drugging the 'undruggable' cancer targets. Nat Rev Cancer. 2017 Aug;17(8):502-508. doi: 10.1038/nrc.2017.36. Epub 2017 Jun 23. PMID: 28643779; PMCID: PMC5945194.

[2] Békés, M., Langley, D.R. & Crews, C.M. PROTAC targeted protein degraders: the past is prologue. Nat Rev Drug Discov 21, 181–200 (2022). https://doi.org/10.1038/s41573-021-00371-6

[3] Mariell Pettersson, Craig M. Crews, PROteolysis TArgeting Chimeras (PROTACs) — Past, present and future, Drug Discovery Today: Technologies, Volume 31, 2019, Pages 15-27, ISSN 1740-6749, https://doi.org/10.1016/j.ddtec.2019.01.002

[4] Deshaies, R. Prime time for PROTACs. *Nat Chem Biol* **11**, 634–635 (2015). https://doi.org/10.1038/nchembio.1887

[5] Pike A, Williamson B, Harlfinger S, Martin S, McGinnity DF. Optimising proteolysis-targeting chimeras (PROTACs) for oral drug delivery: a drug metabolism and pharmacokinetics perspective. Drug Discov Today. 2020 Oct;25(10):1793-1800. doi: 10.1016/j.drudis.2020.07.013. Epub 2020 Jul 18. PMID: 32693163.

[6] https://ir.arvinas.com/news-releases/news-release-details/arvinas-protacr-protein-degrader-bavdegalutamide-arv-110/

[7] Yedla P, Babalghith AO, Andra VV, Syed R. PROTACs in the Management of Prostate Cancer. Molecules. 2023 Apr 25;28(9):3698. doi: 10.3390/molecules28093698. PMID: 37175108; PMCID: PMC10179857.

[8] Chirnomas, D., Hornberger, K.R. & Crews, C.M. Protein degraders enter the clinic — a new approach to cancer therapy. Nat Rev Clin Oncol 20, 265–278 (2023). https://doi.org/10.1038/s41571-023-00736-3

[9] Riching KM, Caine EA, Urh M, Daniels DL. The importance of cellular degradation kinetics for understanding mechanisms in targeted protein degradation. Chem Soc Rev. 2022 Jul 18;51(14):6210-6221. doi: 10.1039/d2cs00339b. PMID: 35792307.

[10] Alber AB, Suter DM. Dynamics of protein synthesis and degradation through the cell cycle. Cell Cycle. 2019 Apr;18(8):784-794. doi: 10.1080/15384101.2019.1598725. Epub 2019 Mar 30. PMID: 30907235; PMCID: PMC6527273.

[11] Tuntland T, Ethell B, Kosaka T, Blasco F, Zang RX, Jain M, Gould T, Hoffmaster K. Implementation of pharmacokinetic and pharmacodynamic strategies in early research phases of drug discovery and development at Novartis Institute of Biomedical Research. Front Pharmacol. 2014 Jul 28;5:174. doi:10.3389/fphar.2014.00174. PMID: 25120485; PMCID: PMC4112793

[12] Grant, J., Hua, F., Apgar, J. F., Burke, J. M., & Marcantonio, D. H. (2023). Mechanistic PK/PD modeling to address early-stage biotherapeutic dosing feasibility questions. mAbs, 15(1). https://doi.org/10.1080/19420862.2023.2192251

[13] Yuan Fang, Shuhang Wang, Songzhe Han, Yizhou Zhao, Cunjing Yu, Huaqing Liu, Ning Li. Targeted protein degrader development for cancer: advances, challenges, and opportunities, Trends in Pharmacological Sciences. Volume 44, Issue 5, 2023. Pages 303-317. ISSN 0165-6147. https://doi.org/10.1016/j.tips.2023.03.003.

[14] Sardu, M.L., Poggesi, I. & De Nicolao, G. Biomarker- versus drug-driven tumor growth inhibition models: an equivalence analysis. J Pharmacokinet Pharmacodyn 42, 611–626 (2015). https://doi.org/10.1007/s10928-015-9427-z

[15] Yates JWT, Holt SV, Logie A, Payne K, Woods K, Wilkinson RW, Davies BR, Guichard SM. A pharmacokinetic-pharmacodynamic model predicting tumour growth inhibition after intermittent administration with the mTOR kinase inhibitor AZD8055. Br J Pharmacol. 2017 Aug;174(16):2652-2661. doi: 10.1111/bph.13886. Epub 2017 Jul 6. PMID: 28556895; PMCID: PMC5522991.

[16] Simeoni M, Magni P, Cammia C, De Nicolao G, Croci V, Pesenti E, Germani M, Poggesi I, Rocchetti M. Predictive pharmacokinetic-pharmacodynamic modeling of tumor growth kinetics in xenograft models after administration of anticancer agents. Cancer Res. 2004 Feb 1;64(3):1094-101. doi: 10.1158/0008-5472.can-03-2524. PMID: 14871843.

[17] Floriane Lignet, Christina Esdar, Gina Walter-Bausch, Manja Friese-Hamim, Sofia Stinchi, Elise Drouin, Samer El Bawab, Andreas D. Becker, Claude Gimmi, Michael P. Sanderson and Felix Rohdich. Translational PK/PD Modeling of M3258. Journal of Pharmacology and Experimental Therapeutics January 1, 2023, 384 (1) 163-172; DOI: https://doi.org/10.1124/jpet.122.001355

[18] FDA. Optimizing the dosage of human prescription drugs and biological products for the treatment of oncologic diseases. *fda.gov*, https://www.fda.gov/regulatory-information/search-fda-guidance-documents/optimizing-dosage-human-prescription-drugs-and-biological-products-treatment-oncologic-diseases (FDA, 2023).

[19] Guzzetti S, Morentin Gutierrez P. An integrated modelling approach for targeted degradation: insights on optimization, data requirements and PKPD predictions from semi- or fully-mechanistic models and exact steady state solutions. J Pharmacokinet Pharmacodyn. 2023 Oct;50(5):327-349. doi: 10.1007/s10928-023-09857-9. Epub 2023 Apr 29. PMID: 37120680; PMCID: PMC10460745.

[20] Gabrielsson J, Peletier LA, Hjorth S. In vivo potency revisited - Keep the target in sight. Pharmacol Ther. 2018 Apr;184:177-188. doi: 10.1016/j.pharmthera.2017.10.011. Epub 2017 Oct 10. PMID: 29024741.

[21] Abbiati RA, Pourdehnad M, Carrancio S, Pierce DW, Kasibhatla S, McConnell M, Trotter MWB, Loos R, Santini CC, Ratushny AV. Quantitative Systems Pharmacology Modeling of Avadomide-Induced Neutropenia Enables Virtual Clinical Dose and Schedule Finding Studies. AAPS J. 2021 Aug 27;23(5):103. doi: 10.1208/s12248-021-00623-8.

[22] A. Alard, O. Katsara, T. Rios-Fuller, C. de la Parra, U. Ozerdem, A. Ernlund, R. J. Schneider. Breast cancer cell mesenchymal transition and metastasis directed by DAP5/eIF3d-mediated selective mRNA translationCell Rep. 2023 June 27; 42(6): 112646. doi:10.1016/j.celrep.2023.112646.

[23] Waters NJ, Jones R, Williams G, Sohal B. Validation of a rapid equilibrium dialysis approach for the measurement of plasma protein binding. J Pharm Sci. 2008 Oct;97(10):4586-95. doi: 10.1002/jps.21317. PMID: 18300299.

[24] Donglu Zhang, Cornelis E.C.A. Hop, Gabriela Patilea-Vrana, Gautham Gampa, Herana Kamal Seneviratne, Jashvant D. Unadkat, Jane R. Kenny, Karthik Nagapudi, Li Di, Lian Zhou, Mark Zak, Matthew R. Wright, Namandjé N. Bumpus, Richard Zang, Xingrong Liu, Yurong Lai and S. Cyrus Khojasteh. Tissue Drug Concentrations: Beyond the Free Drug Hypothesis. Drug Metabolism and Disposition October 1, 2019, 47 (10) 1122-1135; DOI: https://doi.org/10.1124/dmd.119.086744

[25] T. Sobierajski, J. Małolepsza, M. Pichlak, E. Gendaszewska-Darmach, K. M. Błażewska. The impact of E3 ligase choice on PROTAC effectiveness in protein kinase degradation. Drug Discovery Today, Volume 29, Issue 7, 2024

[26] Grime KH, Barton P, McGinnity DF. Application of in silico, in vitro and preclinical pharmacokinetic data for the effective and efficient prediction of human pharmacokinetics. Mol Pharm. 2013 Apr 1;10(4):1191-206. doi: 10.1021/mp300476z. Epub 2013 Jan 29. PMID: 23253040.

[27] Michael Davies, Rhys D.O. Jones, Ken Grime, Rasmus Jansson-Löfmark, Adrian J. Fretland, Susanne Winiwarter, Paul Morgan, Dermot F. McGinnity, Improving the Accuracy of Predicted Human Pharmacokinetics:

Lessons Learned from the AstraZeneca Drug Pipeline Over Two Decades, Trends in Pharmacological Sciences, Volume 41, Issue 6, 2020, Pages 390-408, https://doi.org/10.1016/j.tips.2020.03.004.

[28] F. Lombardo, G. Berellini, L. R. Labonte, G. Liang, S. Kim, Systematic Evaluation of Wajima Superposition (Steady-State Concentration to Mean Residence Time) in the Estimation of Human Intravenous Pharmacokinetic Profile, Journal of Pharmaceutical Sciences, Volume 105, Issue 3, 2016; DOI: https://doi.org/10.1016/S0022-3549(15)00174-4.

[29] Fonsi M, Orsale MV, Monteagudo E. High-throughput microsomal stability assay for screening new chemical entities in drug discovery. J Biomol Screen. 2008 Oct;13(9):862-9. doi: 10.1177/1087057108323911. Epub 2008 Sep 23. PMID: 18812573.

[30] Emmerich, C.H., Gamboa, L.M., Hofmann, M.C.J. et al. Improving target assessment in biomedical research: the GOT-IT recommendations. Nat Rev Drug Discov 20, 64–81 (2021). https://doi.org/10.1038/s41573-020-0087-3

[31] Junfei Cheng, Guoqiang Dong, Wei Wang, Chunquan Sheng. Precise Modulation of Protein Degradation by Smart PROTACs. ChemBioChem 2024, e202400682.. https://doi.org/10.1002/cbic.202400682

[32] Tukey, John W (1977). *Exploratory Data Analysis*. Addison-Wesley. ISBN 978-0-201-07616-5. OCLC 3058187.

[33] Jakob M. Bader, Vincent Albrecht, Matthias Mann, MS-Based Proteomics of Body Fluids: The End of the Beginning, Molecular & Cellular Proteomics, Volume 22, Issue 7, 2023, https://doi.org/10.1016/j.mcpro.2023.100577.

[34] E. M. Tosca, D. Ronchi, M. Rocchetti, P. Magni. Predicting Tumor Volume Doubling Time and Progression-Free Survival in Untreated Patients from Patient-Derived-Xenograft (PDX) Models: A Translational Model-Based Approach. AAPS Journal (2024) 26:92

[35] Betts A, Clark T, Jasper P, Tolsma J, van der Graaf PH, Graziani EI, Rosfjord E, Sung M, Ma D, Barletta F. Use of translational modeling and simulation for quantitative comparison of PF-06804103, a new generation HER2 ADC, with Trastuzumab-DM1. J Pharmacokinet Pharmacodyn. 2020 Oct;47(5):513-526. doi: 10.1007/s10928-020-09702-3. Epub 2020 Jul 24. PMID: 32710210; PMCID: PMC7520420.

Fig. 1 Translational PK/PD framework for target protein degraders

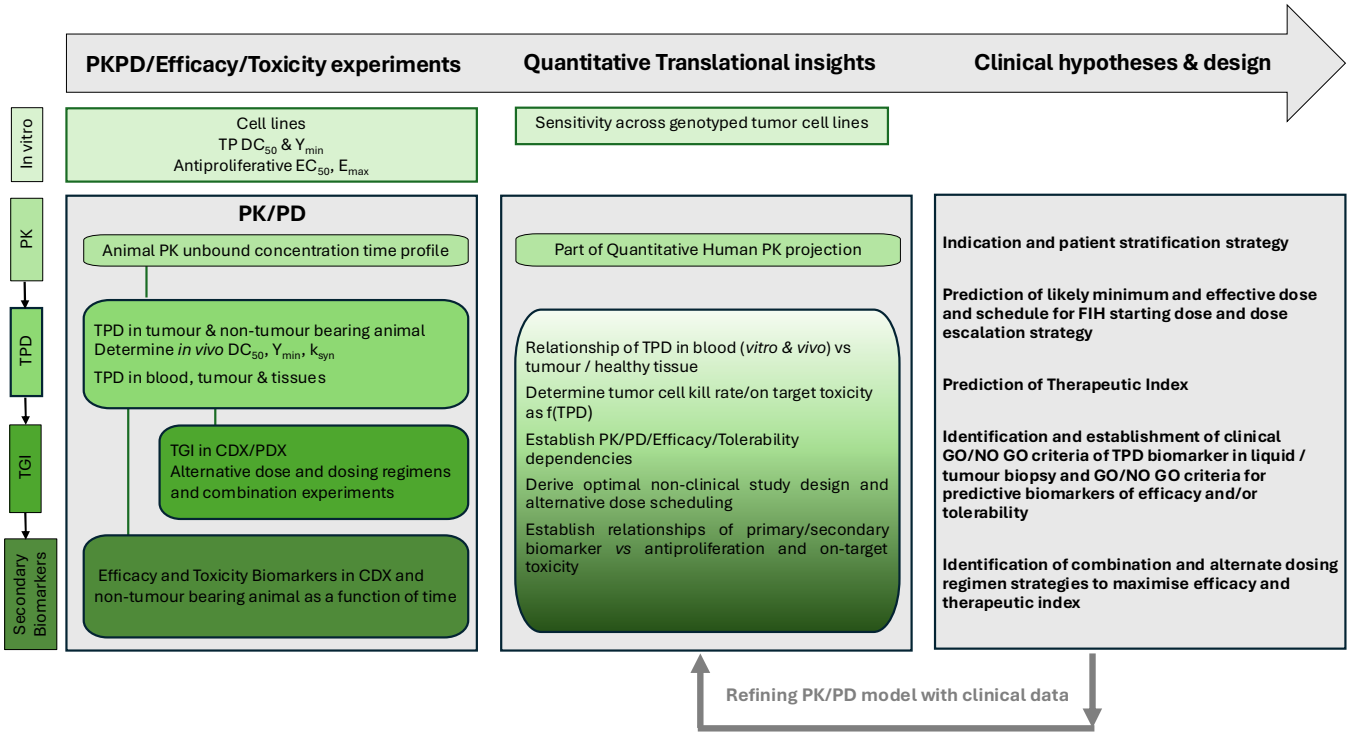


Fig 1: Translational PK/PD framework for target protein degraders

Key model parameters needed to simulate efficacy and safety of new TPD can be estimated from in vitro assays and in vivo animal models. This scheme represents the information flow driven by the described modelling paradigm and pre-clinical in vitro and in vivo data collection, translational approaches and selected model informed clinical variables. Among the different observables: The drug PK is assumed to impact directly the modulation of the target protein (TP), while the residual TP level is assumed to directly influence the tumor killing rate (efficacy outcome) and the turnover of additional secondary biomarkers included as on-target dependent observables in the experimental design.

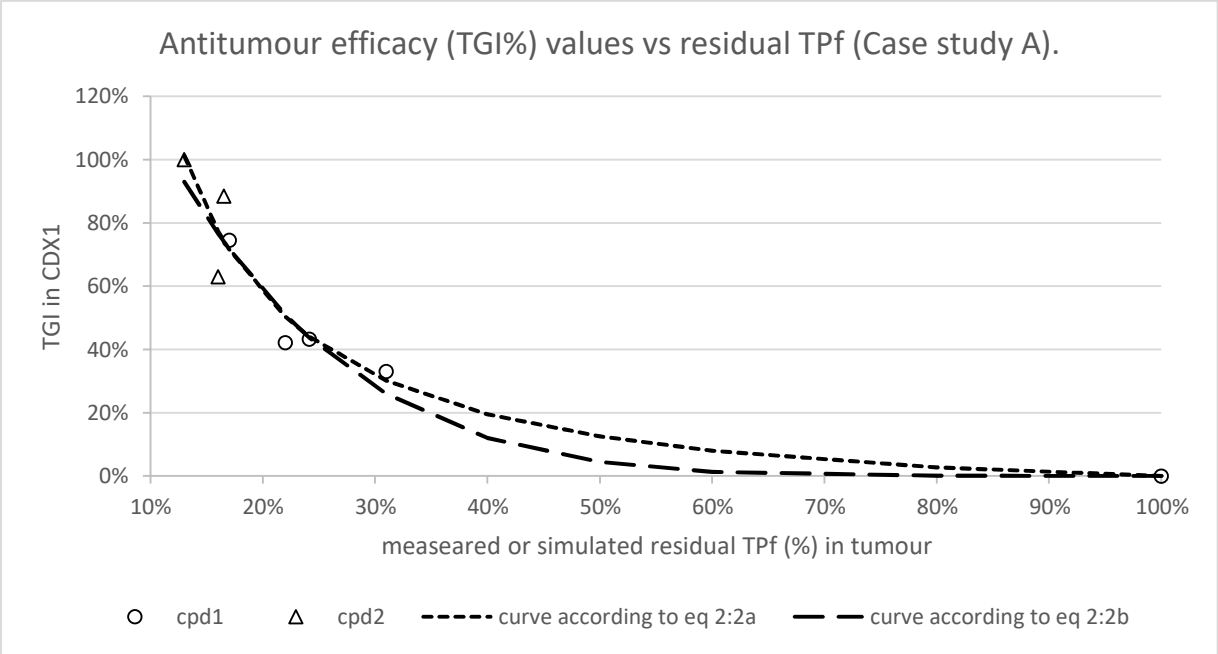
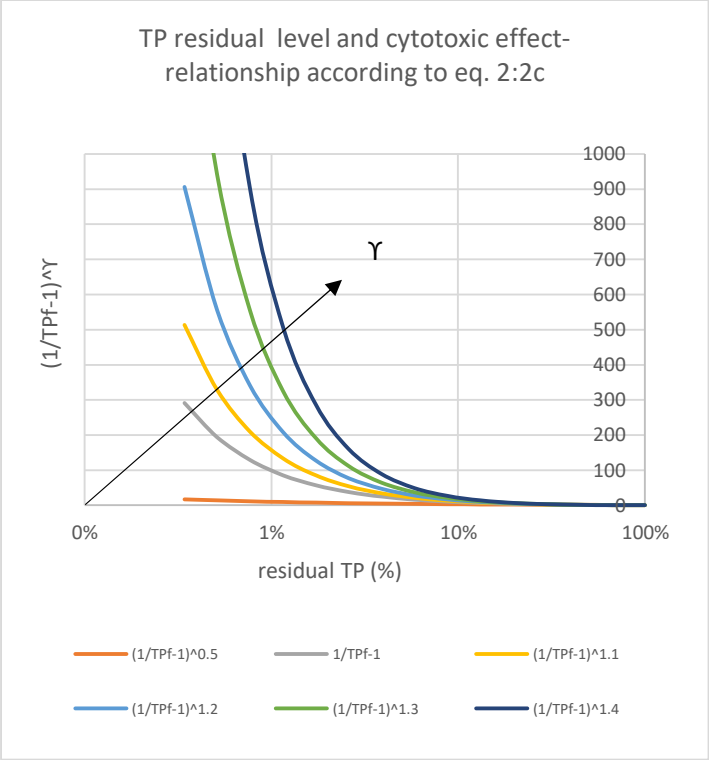


Fig 2: Antitumour efficacy (TGI%) values vs residual TPf (Case study A).

Dots in this plot represent the experimentally evaluated effect (TGI) at the end of treatment vs. the measured TPf (%) (average of measured values, within the dosing interval, post last administration). Experimental data refer to compounds 1 and 2 tested in CDX1. Curves obtained using eq. 2:2a and 2:2b have been plotted for comparison.



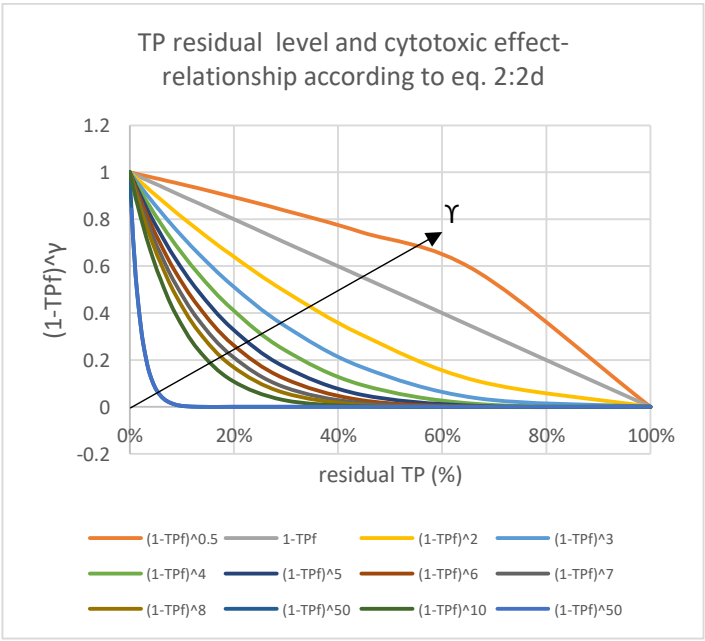


Fig 3: Examples of f_{TGI}(TPf) functions:

These plots exemplify the impact of the equation chosen to represent the quantitative relationship between TP degradation and cytotoxic effect (i.e. relative tumour killing rate). To show the impact of gamma parameter on the curve shape, in fig. 3a the plotted lines are based on eq. 2:2c using different values for gamma. In fig. 3b, the plotted lines are based on eq. 2:2d using different values for gamma.

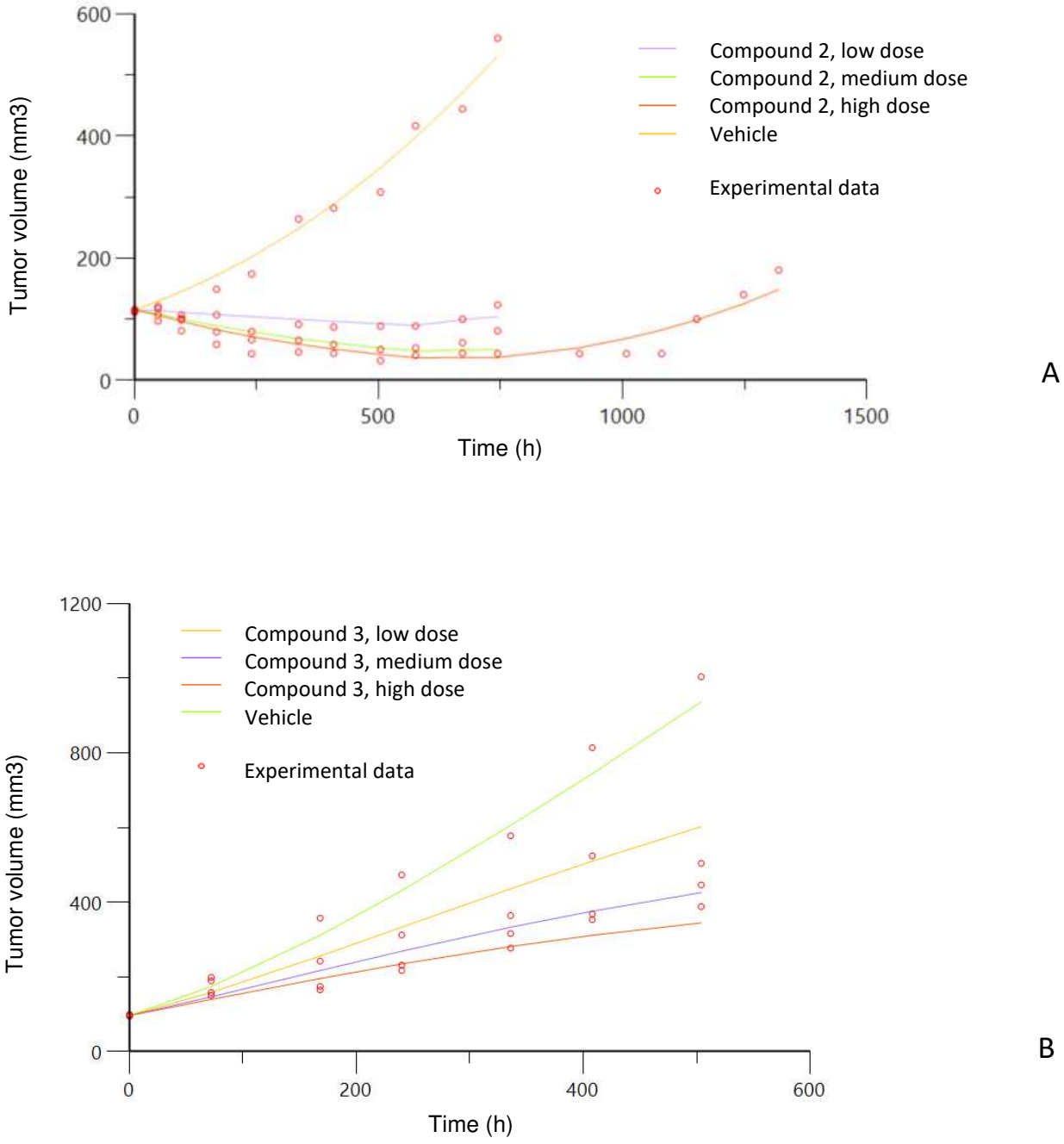
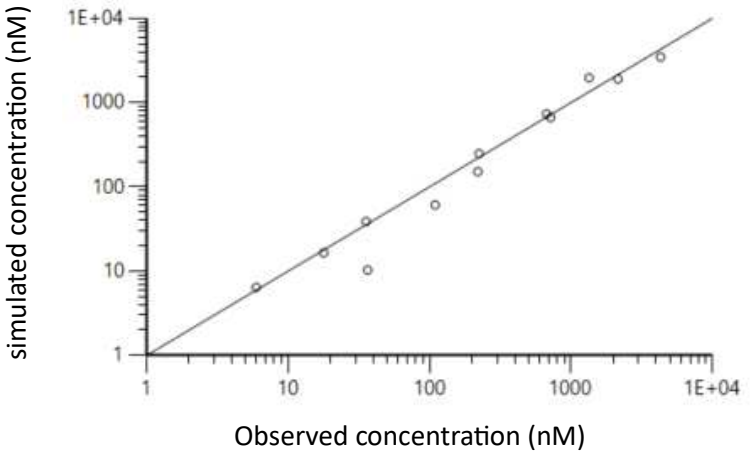
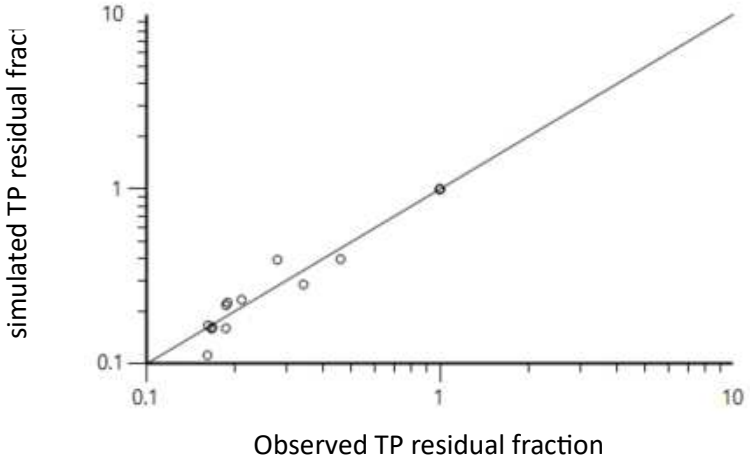


Fig 4: Model simulated vs experimentally measured tumour volumes with time A) CDX1 ; B) CDX2. (case study A)

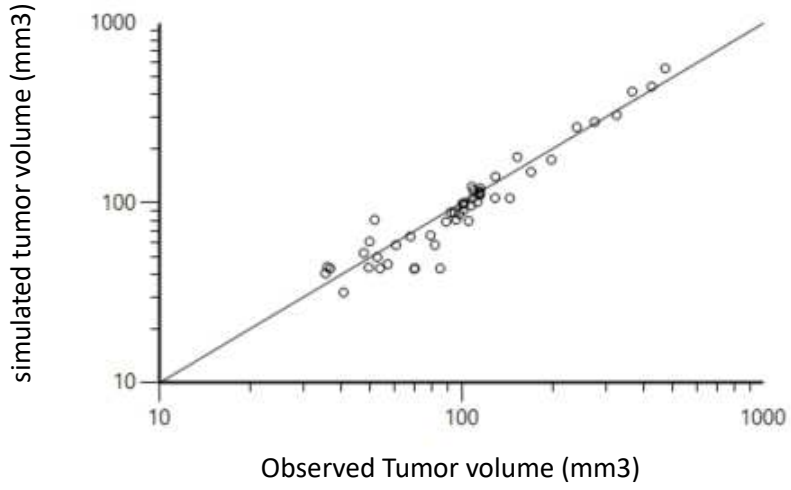
Tumour volumes were simulated using the model equations described in main text (continuous lines), while dots represent experimentally measured values. The same model equations were used to fit the experimental data in fig 4a and 4b, generated using a different CDX and compound combination in each experiment (but the degraded TP was the same). Equation parameters were different for each CDX and estimated by Phoenix to minimize the differences between simulated and measured tumour volumes.



A



B



C

Fig 5: Experimentally measured and model simulated values for drug concentration (C), TPf and tumour volume (TV): CDX model 1 - case study A (Fig. 4A).

These plots refer to all the observables (compound concentration in plasma, TPf, and tumour volume) collected testing compound 2 in CDX1 (see also fig. 4A). The straight lines represent the linear curves correlating the measured values and the model estimations for each observable.

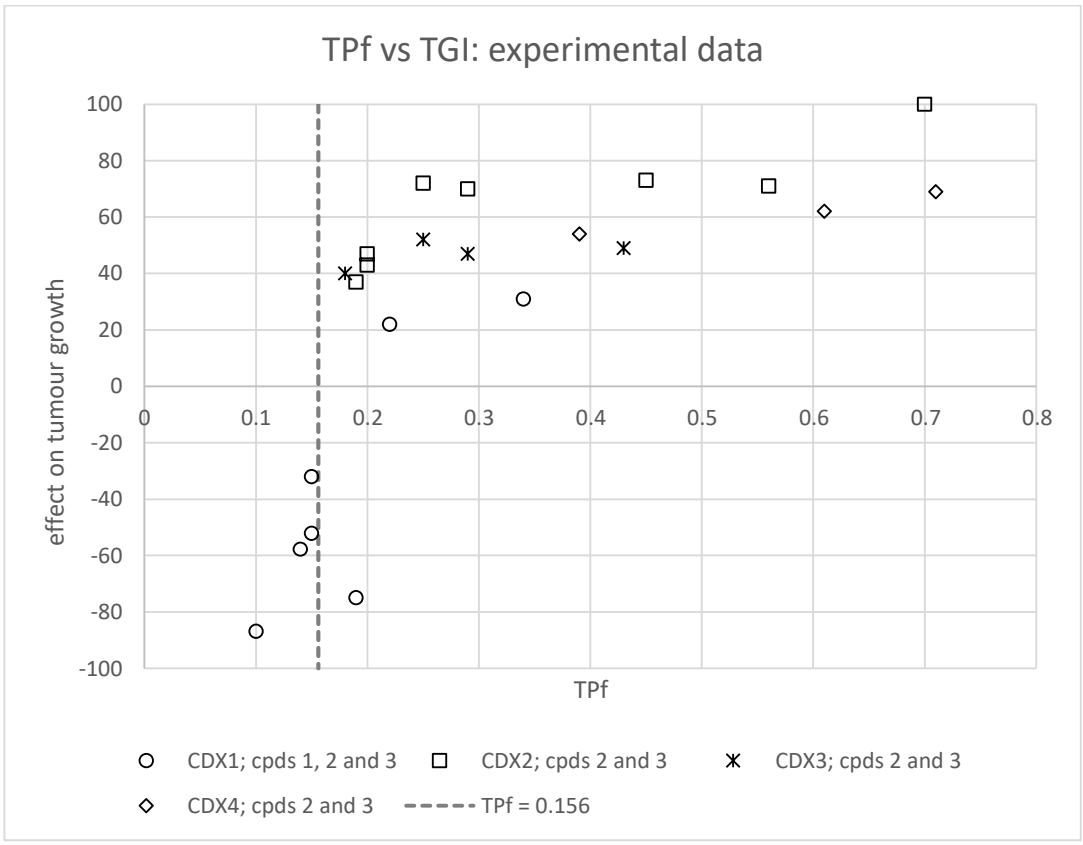


Figure 6: Global effect on tumour growth in case study A.

Global correspondence between TP degradation and tumour growth, with different CDX models and TPDs.

Effect on tumour growth was expressed differently depending on if the compound effect consisted of a reduction in growth rate or if the effect caused tumour growth regression.

For tumour growth rate reduction, (i.e. when $T(treatment)_f > T(treatment)_i$) the effect was expressed as:

$$\frac{T(treatment)_f - T(treatment)_i}{T(vehicle)_f - T(vehicle)_i} * 100 \quad (2{:}1\ a)$$

For tumour growth regression, (i.e. when $T(treatment)_f < T(treatment)_i$) the effect was expressed as:

$$\frac{T(treatment)_f - T(treatment)_i}{T(vehicle)_i} * 100 \quad (2{:}1\ b)$$

Where T is tumour size, in parenthesis it is specified if the value refers to the vehicle or the drug treated group, the subscript "*i*" refers to the initial (day 1 of treatment) or final "*f*" (last day of treatment) tumour volume measurement.

Considering that $T(treatment)_i$ is approximately equal to $T(vehicle)_i$, the lower is the value estimated according to equations 2:1, the stronger is the efficacy: positive values correspond to simple growth inhibition, while tumour regression generates negative values. A result close to 100% corresponds to no growth inhibition effect, 0% corresponds to tumour stasis ($T(treatment)_f = T(treatment)_i$), -100% indicates total tumour regression.

TPf = 0.156 (indicated by the vertical dotted line crossing the X axis) represents the threshold value that according to the model equations predicts an effect of at least tumour stasis (see text for further details).

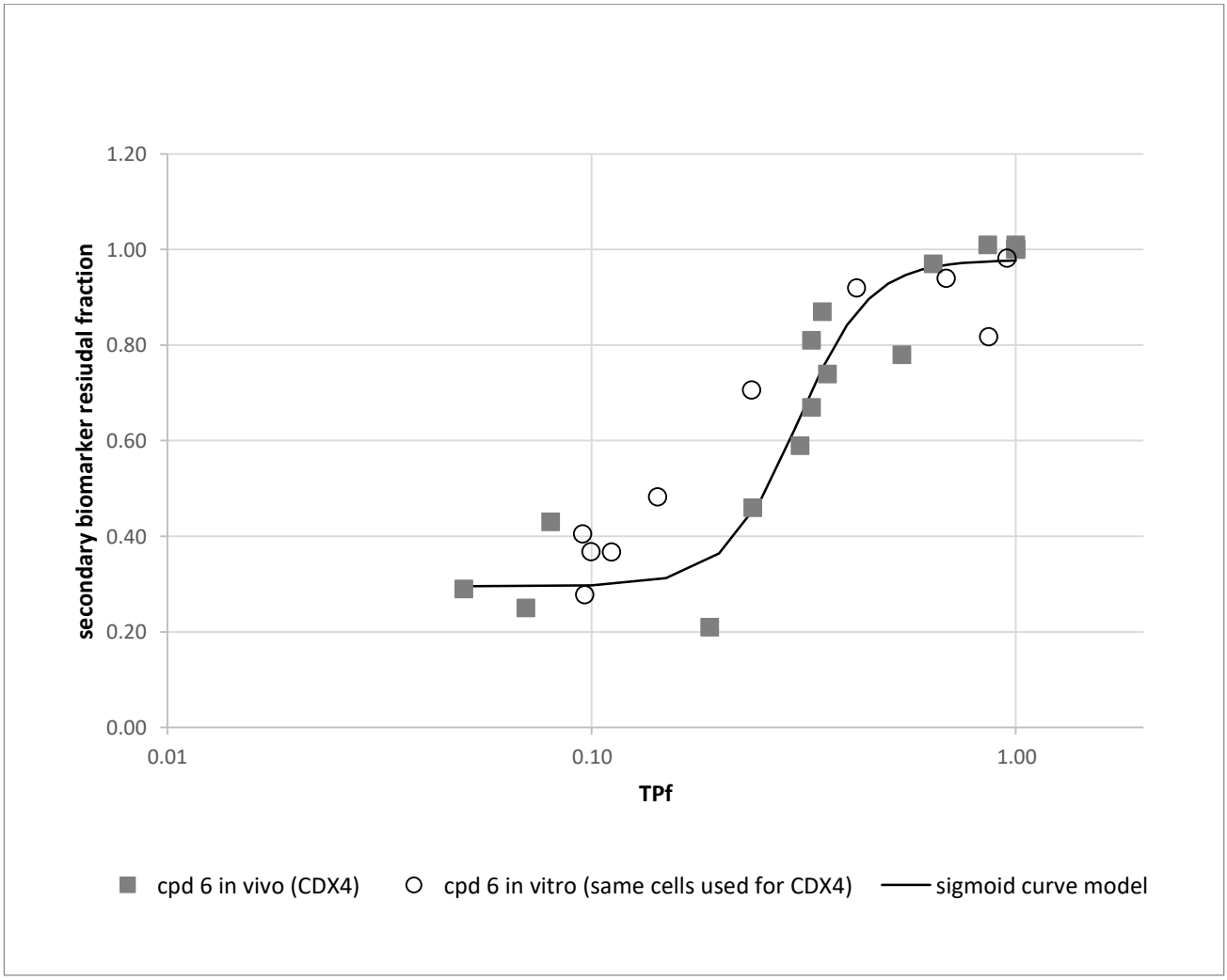
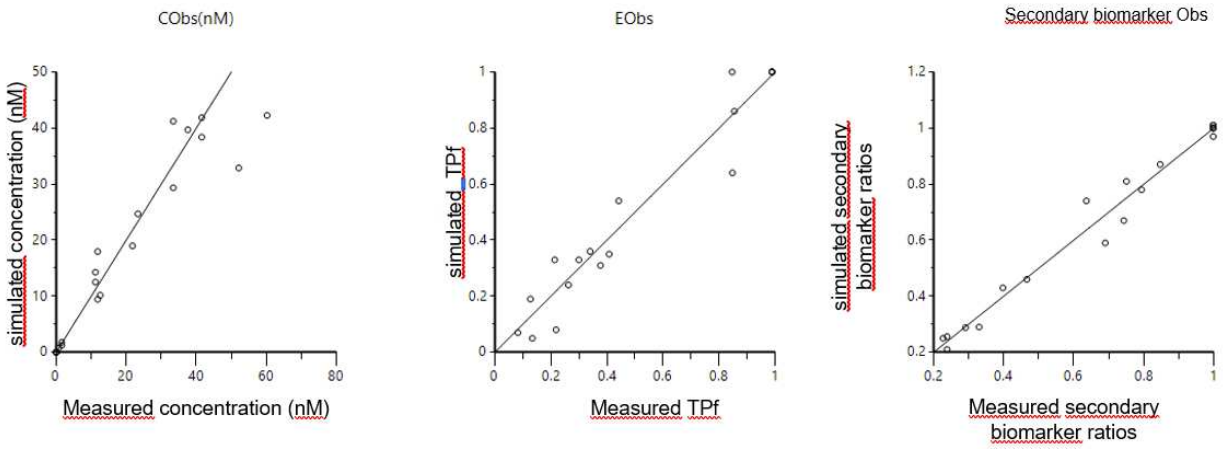
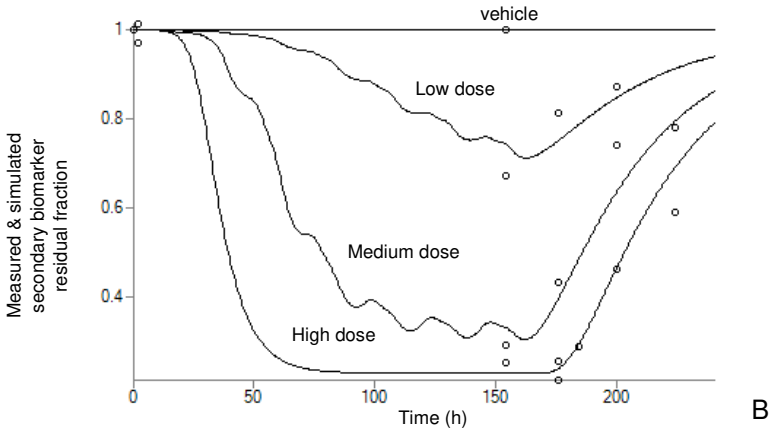


Figure 7: Secondary biomarker vs. TPf in vitro and in vivo measured values for Compound 6 in CDX4 (Case study B).

The sigmoid curve represents the interpolation between measured secondary biomarker residual fractions and the corresponding estimations based on eq. 3:3, using TPf as input.



A



B

Figure 8: Model fitted data vs. experimental measures (Case study B):

A: These plots refer to all the observables (compound concentration in plasma, TPf, and secondary biomarker modulation) collected testing compound 6 in CDX4. The straight lines represent the linear curves correlating the measured values and the model estimations for each observable.

B: Model simulated (continuous lines) vs experimentally measured secondary biomarker residual fractions (dots) with time (testing compound 6 in CDX4).

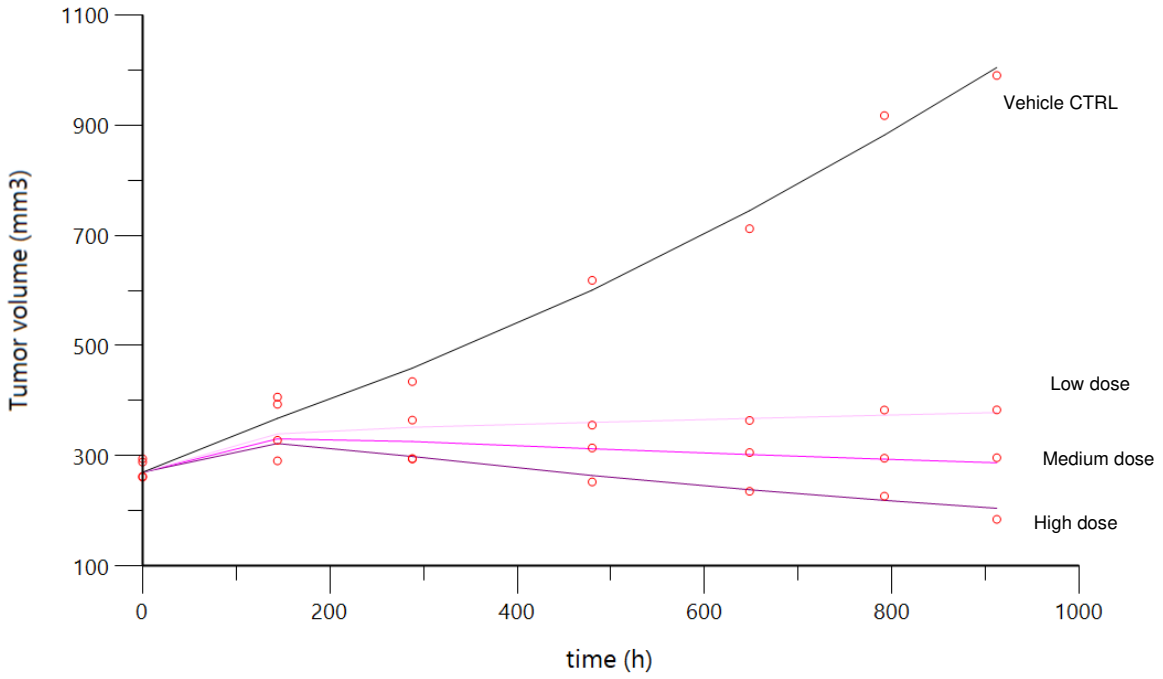


Figure 9: Tumor growth vs time – Compound 6 in CDX4 (Case study B):

Tumour volumes were simulated using the model equations described in the main text (continuous lines), while dots represent experimentally measured values.

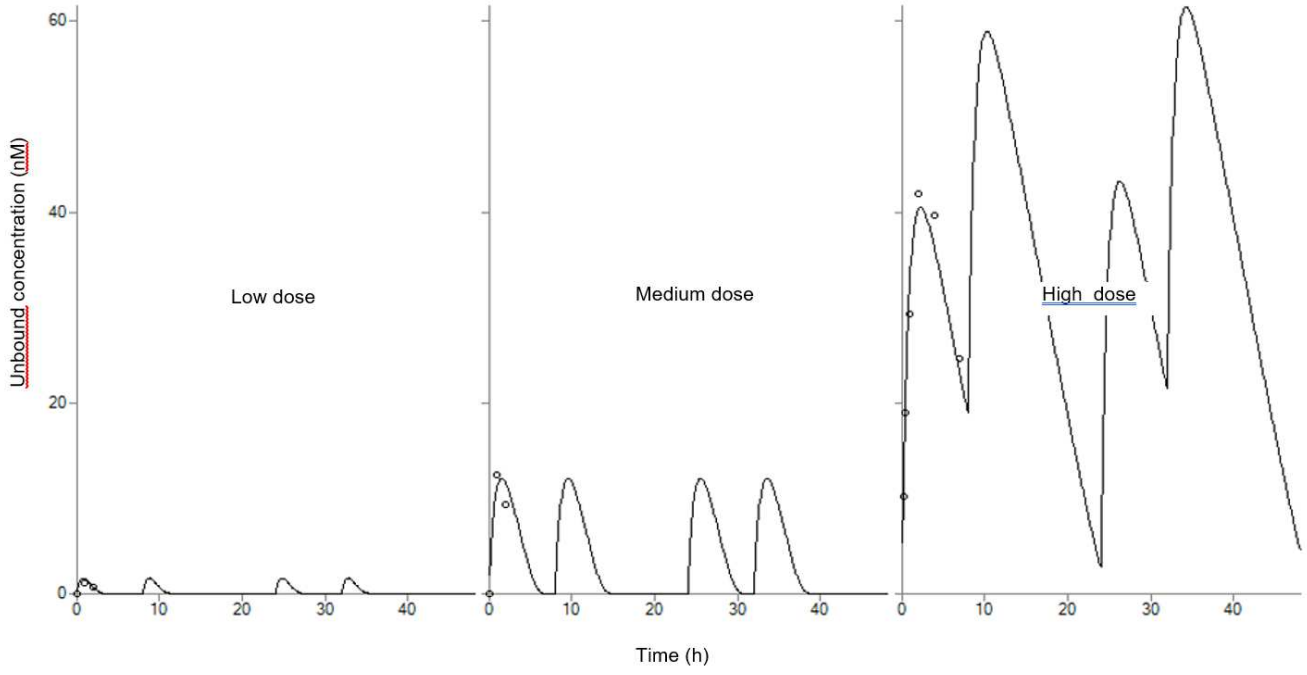


Figure 9b: Plasma unbound concentration vs time – Compound 6 in CDX4 (Case study B):

Concentrations were simulated using saturable clearance to account for the more than dose proportional increase in exposure, while dots represent experimentally measured values. Dose relative ratios were 1:4:10 for low:medium:high respectively

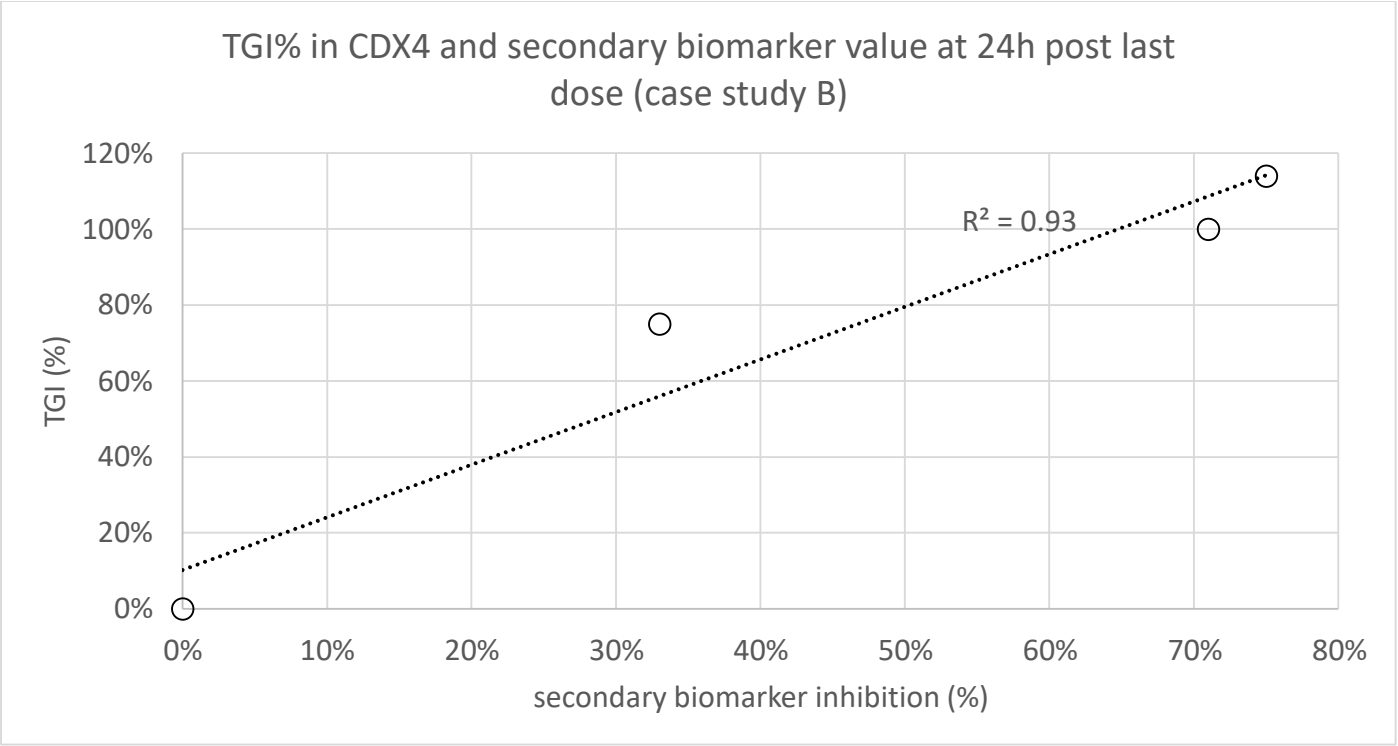


Figure 10: TGI% in CDX4 and secondary biomarker value at 24h post last dose (case study B)

Secondary biomarker inhibition (values measured in tumours at 24h post last administered dose) and TGI% values at the end of treatments, observed with compound 6 in CDX4. The plotted straight line represents the best linear curve interpolating the experimental values (Case study B):

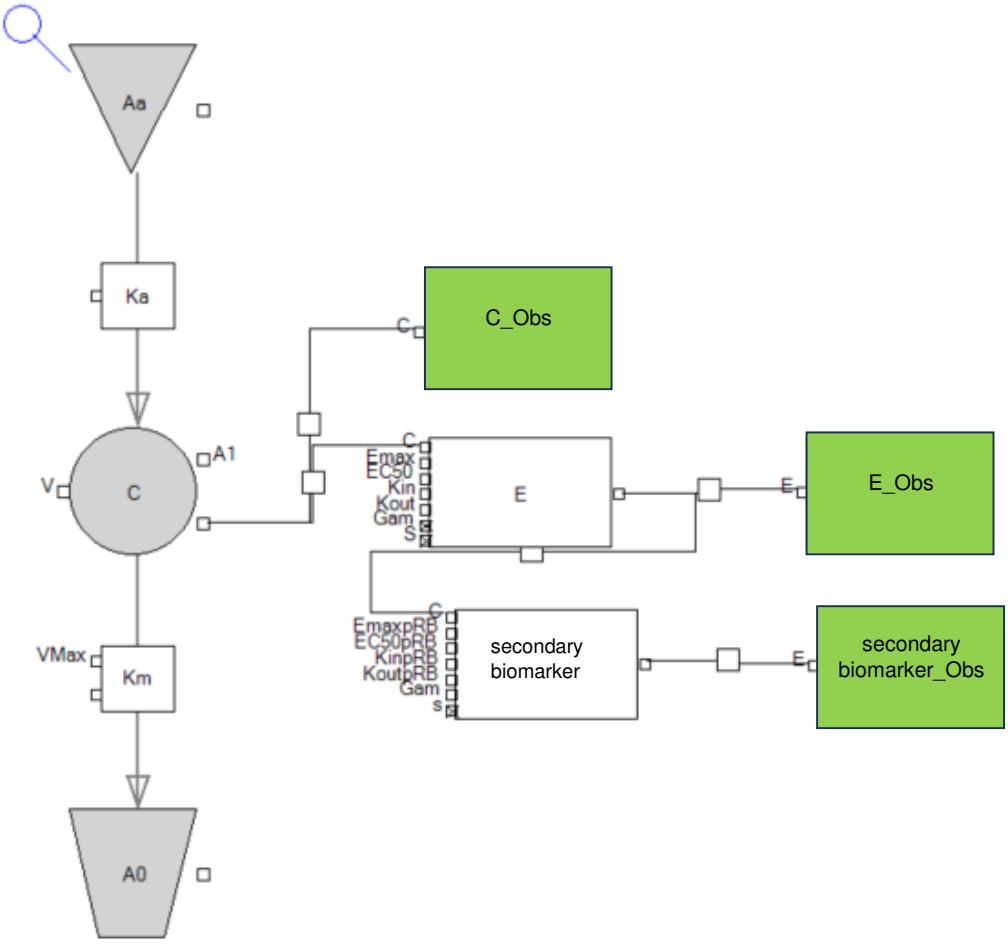


Figure 11: Model used for the 7-days PK/PD study - Case study B:

Tumors volume is not recorded during this short study. The simplified model structure is visually represented via the graphical interface in Phoenix.

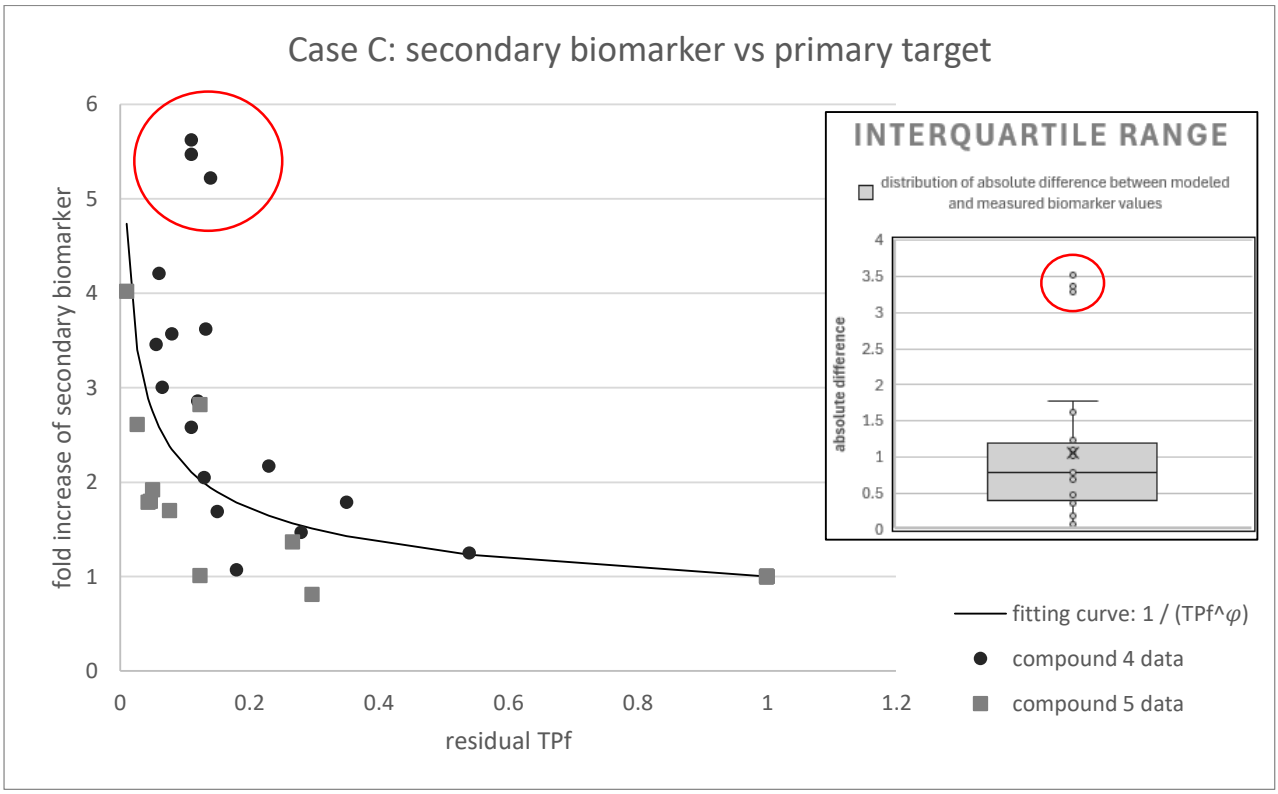


Figure 12: Relationship between target protein degradation (TPf) and secondary biomarker (study case C):

Data refer to two different TPD compounds (compounds 4 and 5) targeting the same protein in tumours collected from CDX5. Inlet plot: absolute residual differences (predicted values using the equation: 1 / (TPf^φ) – measured values) spread using the interquartile range plot analysis. Data circled in red are considered potential outliers compared to the fitting curve.

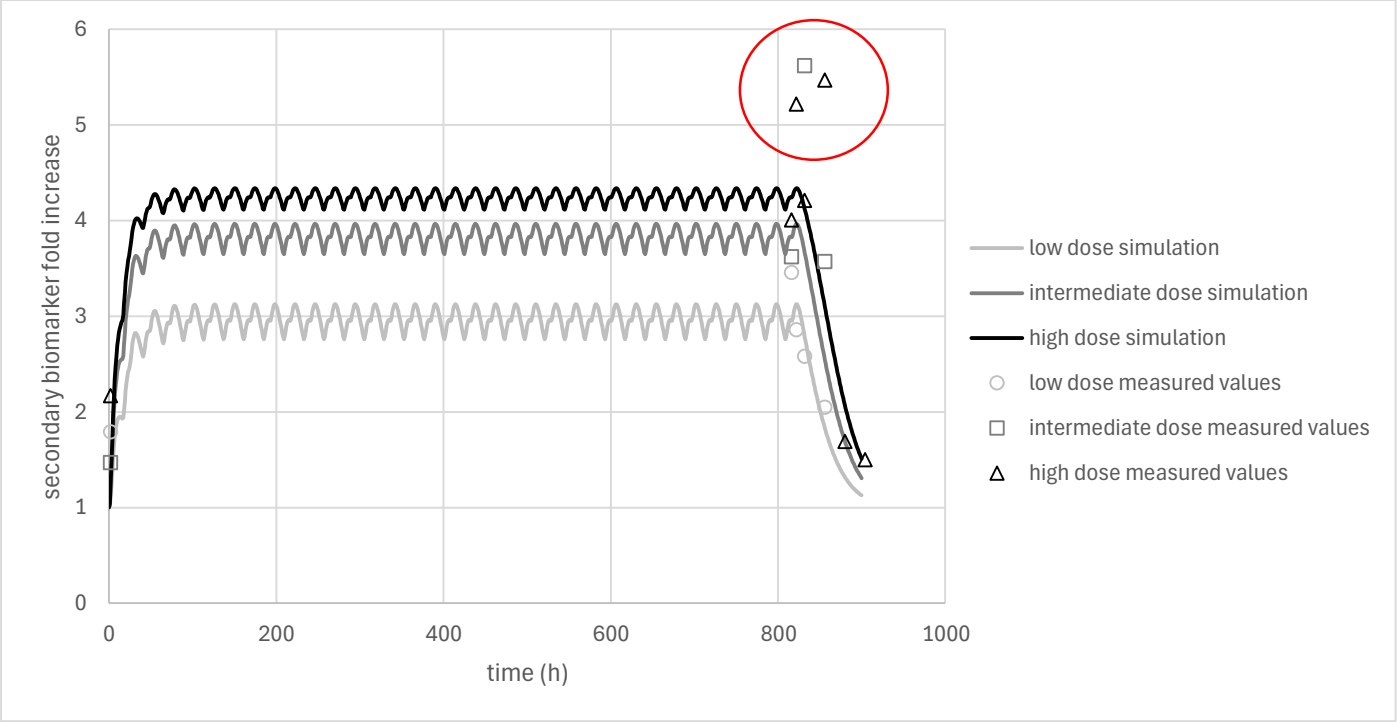


Figure 13: Simulated vs measured levels of the secondary biomarker with time (study case C): Circled data are considered potential outliers (see also fig. 12 and main text).

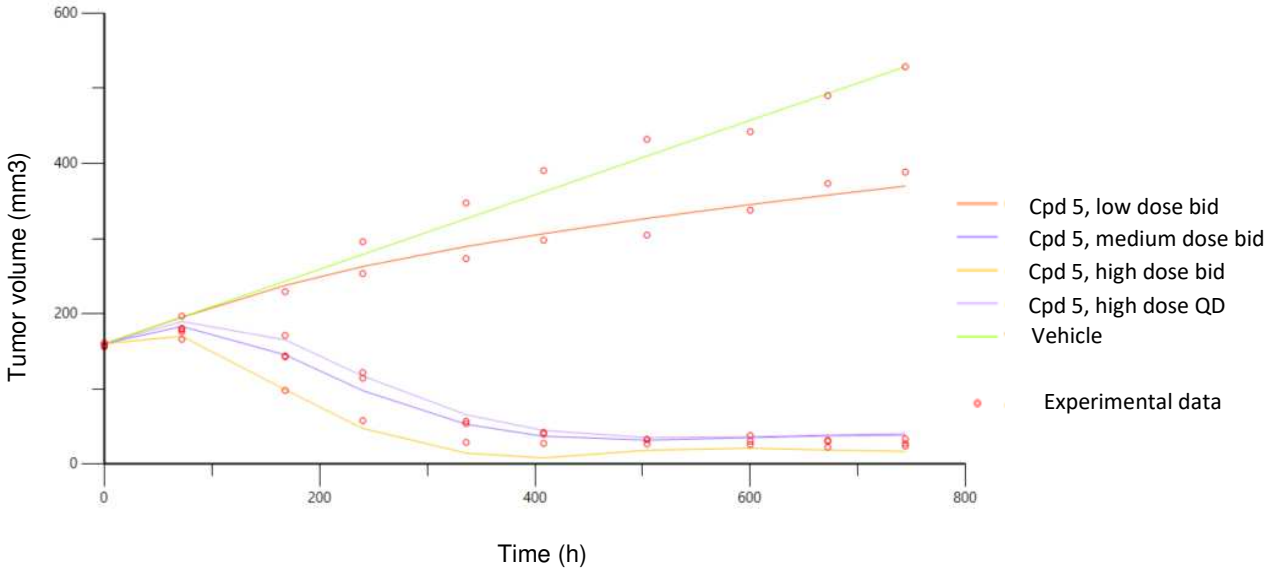


Figure 14: Model simulated vs experimentally measured tumour volumes with time (case study C).

Tumour volumes from CDX5 mice were simulated using the model equations described in main text (continuous lines), while dots represent experimentally measured values. Different doses and, at the high dose, different administration regimens (b.i.d. and q.d.) were tested in parallel. Equation parameters were assumed the same for all the treated groups and were estimated by minimizing the differences between simulated and measured observables.

TABLES

Table1: in vivo PK/PD parameters (case study A).

	Compound tested, CDX model		PK/PD in NHP (in vivo PBMCs)	
	cpd 2, CDX 1	**cpd 3, CDX 2**	**cpd 3**	
Parameter	**Estimate (CV%)**	**Estimate (CV%)**	**Estimate****	**Units**
ksyn /[TP0]	0.10 (20%)	0.039 (24%)	0.15 – 0.005***	1/h
kdeg	0.10 (20%)	0.039 (24%)	0.15 – 0.005***	1/h
Emax / Ymin (%)	4.9 / 17.7% (12%)	4.3 / 19.1% (33%)	32 / 3%	-
EC50u	44 (24%)	3 (68%)	2.3****	nM
L0	0.0029 (12%)	0.013 (26%)	NA	1/h
L1	1.89 (33%)	2.75 (42%)	NA	$(mm^3)/h$
k2	3.39E-05 (48%)	3.94E-06 (39%)	NA	1/h
k1*	1 (NA)	1 (NA)	NA	1/h
gamma	3.2 (24%)	4.8 (44%)	NA	-

*k1 was kept frozen
** averaged values from all animals
*** range of values measured in individual animals
**** in vitro DC50 in human and in NHP PBMCs were respectively 0.5nM and 0.6nM (average of 6 donors per species); range of values in human: 0.4 – 0.8 nM , range of values in NHP: 0.2 – 1.0 nM

Table2: Sigmoid function parameters estimated in fig.7 (case study B)

Sigmoid function parameters estimated in fig.7 (case study B)

Parameter	Estimate	Stderr	CV%
$tvEC50_2$	0.306	0.0132	4.33
$tvGam_2$	6.25	2.10	33.5
tvE0	0.296	0.0393	13.3
$tvEmax_2$	0.683	0.0503	7.38
stdev0	0.0743	0.0124	16.7

Table3a

In vitro & in vivo PD model parameters comparison for case study B

	Tumour cells used in CDX4				**NHP PKPD (in vivo PBMCs)**	**Dog PKPD (in vivo PBMCs)**
	in vitro Hibit 4h	**in vitro Hibit 24h**	**in vitro quantitative protein analysis**	**CDX4 in vivo***		
Ymin (%)	na	na	1.6	3.4	1.8	0.9
$DC50_u$ (nM)**	0.23	0.09	0.10	0.08	0.22	3.3
ksyn/$[TP_0]$ (1/h)	na	na	na	0.008	0.006	0.023

DC50 *in vitro* ratio in human PBMCs/ NHP PBMCs / dog PBMCs : 1:1:10 (see also table 3b).

In vitro & in vivo PD parameters comparison for case study B

*Model estimated tumour stasis (based on eq 1:4b to 1:4m and eq. 2:2d and 2:2e) is achieved at TPf = 0.04 (TPf % = 4%)

**DC50 values were corrected for the unbound fraction estimated by micro-dialysis in the medium used for cell culture (in vitro) or in plasma (in vivo)[23].

Table 3b

Measured target protein degradation parameters in vitro in PBMCs from different species. Reported values are the average of multiple donors (case study B).

Target species	**DC_{50}* nM**	**Ymin** % **	**n. of analyzed donors**
Human	0.01	7	4
NHP	0.01	4	7
Dog	0.10	5	9
Rat	0.03	10	4
Mouse	NA	25	3

* DC50 estimation was based on nominal spiked concentrations in isolated PBMCs; unbound concentration was not experimentally estimated in isolated PBMCs but assumed identical across all tested species

** Ymin refers to the value at the highest tested concentration (1µM).

Table4a

TPf (%) values measured in rat following 14 days of daily treatment with cpd 6

TP degradation [%]*						
	low dose group		intermediate dose group		high dose group	
Matrix	Male (n=3)	Female (n=3)	Male (n=3)	Female (n=3)	Male (n=3)	Female (n=3)
PBMCs	73	72	92	86	97	98
Spleen	58	63	79	77	89	89
Lung	64	64	82	71	90	92
Liver	74	73	90	86	94	95
Kidney	69	62	85	78	94	94
Colon	79	79	88	90	94	96
Ileum	91	86	95	89	97	98
Bone Marrow	46	57	54	52	76	87

* averages % estimated comparing residual TP values vs control group (n= 3M & 3F). Tissues were sampled 24h post last administration

Table4b

TPf values measured in dog following 14 days of daily treatment with cpd 6

TP degradation [%]*						
	low dose group		intermediate dose group		high dose group	
Matrix	Male (n=1)	Female (n=1)	Male (n=1)	Female (n=1)	Male (n=1)	Female (n=1)
PBMCs	99	>99.5	99	>99.5	97	>99.5
Spleen	90	63	81	91	90	88
Lung	89	86	83	92	93	94
Liver	92	92	91	95	94	96
Kidney	95	97	96	98	98	99
Colon	98	98	99	99	99	99
Ileum	96	97	99	99	99	99
Bone Marrow	84	94	96	96	97	98

Compared to control group (n= 1M & 1F). Tissues were sampled 24h post last administration

Table5

In vitro & in vivo PD parameters comparison for case study C

	In vitro Dog Hematic Cytotoxicity (Myel/Eryth)*	**In vitro Human Hematic Cytotoxicity (Myel/Eryth)***	**In vitro NHP Hematic Cytotoxicity (Myel/Eryth)***	**CDX5/CDX6 (TPD in tumor)****	**In vivo Dog / NHP PKPD (TPD in PBMCs)****
IC50 or DC50 (nM)	0.13 / 0.18	0.15 / 0.19	37 / 21	16 / 30	6 / na
In vivo Ymin (%)	na	na	na	1.5% / 2%	0.5% / 24%
kin/[TP_0] (1/h)	na	na	na	0.006 / 0.009	0.008 / na

* Cytotoxicity assessed via Cell Titer Glo at Days 7 and 9. In mice and rats IC50 values were ≥ 700nM. Myel = myeloids ; Eryth = erytroids. In vitro IC50 values were estimated using nominal spiked concentrations

**unbound DC50 (estimated from total plasma concentration, corrected for PPB)

DC50 relative ratio: *in vitro* human PBMCs / *in vitro* dog PBMCs / in vitro CDX5 / in vitro CDX6 : 1 : 10 : 1.33 : 1.67 (In vitro DC50 values were estimated using nominal spiked concentrations)